Contrasting effects of increasing irrigation efficiency on hydrological drought based on hydrological scenario simulations

Journal of Hydrology

Cheng, Hui; Wang, Wen; de Graaf, Inge; Lu, Jingxuan; van der Kooij, Saskia et al

https://doi.org/10.1016/j.jhydrol.2024.132261

Journal of Hydrology 645 (2024) 132261

Contents lists available at ScienceDirect

Journal of Hydrology

journal homepage: www.elsevier.com/locate/jhydrol

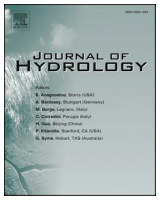

Research papers

Contrasting effects of increasing irrigation efficiency on hydrological drought based on hydrological scenario simulations

Hui Cheng [a,b,c,d], Wen Wang [c,*], Inge de Graaf [e], Jingxuan Lu [b], Saskia van der Kooij [d], Jeroen Vos [d], Yuan Yao [f], Pieter van Oel [d,*]

[a] Yellow River Engineering Consulting Co., Ltd., Zhengzhou 450003, China
[b] Research Center on Flood & Drought Disaster Reduction, China Institute of Water Resources and Hydropower Research, Beijing 100038, China
[c] The National Key Laboratory of Water Disaster Prevention, Hohai University, Nanjing 210098, China
[d] Water Resources Management Group, Wageningen University& Research, P.O. Box 47, 6700 AA Wageningen, the Netherlands
[e] Earth Systems and Global Change Group, Wageningen University& Research, P.O. Box 47, 6700 AA Wageningen, the Netherlands
[f] School of Water Conservancy, North China University of Water Resources and Electric Power, Zhengzhou 450046, China

ARTICLE INFO

Handling Editor: Marco Borga

Keywords:
PCR-GLOBWB 2.0 model
Paradox of irrigation efficiency
Hydrological drought
Huaihe River Basin

ABSTRACT

Over-exploitation of water resources leads to water scarcity and aggravation of hydrological drought. An approach to addressing the problem is to invest in increasing irrigation efficiency (IE). However, higher IE may lead to the paradox of IE, that is, after increasing IE, irrigation water consumption (IWC) could increase rather than decrease. An important cause of the paradox of IE is that increasing IE may lead to an increase in irrigation area (IA). Therefore, an improved understanding of the impacts of such practices on hydrological drought is needed. This study used the PCR-GLOBWB 2.0 model to investigate the effects of increasing IE on hydrological drought for the catchment above Bengbu in the Huaihe River Basin in central eastern China. The hydrological drought was simulated under three scenarios, i.e., a baseline scenario in which IE remains unchanged, an IE increases scenario, and an IE & IA increase scenario. The results show that increasing IE has two contrasting effects: aggravation and alleviation of hydrological drought. For instance, the increase in IE (from 0.562 to 0.601 in Henan, 0.482 to 0.544 in Anhui, and 0.464 to 0.522 in Hubei province) from 2009 to 2019 reduced standardized drought streamflow deficit (SDSD) by about 5 ~ 60 % in the central parts of the study area, whereas in the northern edge of the study area, it intensified SDSD even by more than 80 %. When water availability (WA) is high and can meet most of the crop water demand, increasing IE will lead to a situation in which the increase of IWC is less than the decrease of irrigation water withdrawal (IWW). In this situation, increasing IE alleviates the hydrological drought as intended. However, when water resources are relatively scarce with limited WA and cannot meet most of the crop water demand, increasing IE could lead to a paradoxical situation where the increase of IWC is higher than the decrease of IWW and thereby aggravates the hydrological drought. Also, increasing IE can aggravate the hydrological drought in water-receiving areas by reducing water supply from outside water supply regions. Results show that the impact of increasing IE and IA on hydrological drought is also two-sided, but the aggravating effect is dominant because the increase in IA leads to a significant increase in IWW and IWC. However, when the irrigation system restricts the increase of IA (the IA cannot increase or only slightly), the intensification effect of increasing IE and IA on hydrological drought will be weakened, and may even alleviate the hydrological drought. These results underline the importance of considering consequences at both local and basin scales, particularly for periods during and following drought, when policy makers consider the promotion of water-saving measures at irrigation-system level.

1. Introduction

Drought is one of the disasters that produce the most intense socio-economic impacts (Zhang et al., 2022a). In contrast to other natural disasters, severe droughts can last months to years and spread over large regions (AghaKouchak et al., 2021). Droughts are commonly divided

* Corresponding authors.
E-mail addresses: wangwen@hhu.edu.cn (W. Wang), pieter.vanoel@wur.nl (P. van Oel).

https://doi.org/10.1016/j.jhydrol.2024.132261
Received 12 October 2023; Received in revised form 7 September 2024; Accepted 12 October 2024
Available online 29 October 2024

into meteorological, agricultural, hydrological, and socio-economic droughts. Hydrological drought is usually characterized by negative anomalies of streamflow, which can directly affect municipal, industrial, and agricultural water supply, and hydropower and thermal power generation, which will lead to more significant economic and environmental impacts compared to other types of droughts (Van Loon et al., 2016; Van Langen et al., 2021). In recent years, numerous studies have revealed the significant impact of human water use on hydrological droughts (e.g., He et al., 2017; Van Oel et al.,2018; Yang et al., 2020; AghaKouchak et al.,2021; Cheng et al., 2021; Schilstra et al., 2024). Wada et al. (2013) showed that the drought intensity globally has increased by 10 ~ 500 % due to water use, of which irrigation water use is the main factor. A recent study (Van Loon et al., 2022) conducted on 28 watersheds globally showed that human water withdrawal significantly aggravated the drought characteristics, increased the cumulative drought duration by 20 ~ 305 %, and increased the cumulative drought deficit by nearly 3000 %. People have gradually realized that human water use has exacerbated the water crisis and even worsened the hydrological drought (AghaKouchak et al., 2021; Cheng et al., 2021). In addition, the economic development and the increase of population will further increase the risk of hydrological drought as more water will be consumed in the future (Wanders and Wada, 2015; Yang et al., 2020).

Reconciling limited water resources with higher water use demand is a great policy dilemma for many governments (Grafton et al., 2018). Given that irrigation accounts for 70 % of water withdrawals globally and 40 % of the global surface area is affected by agricultural activities, governments often promote increasing irrigation efficiency (IE). The main measures to improve IE include pipeline technology, canal lining, and the use of water-saving irrigation technologies such as advanced surface irrigation, sprinkler micro-irrigation, and optimization of irrigation district management system. For example, advanced irrigation technologies such as sprinkler or drip irrigation could “save” water, with IE going to 0.9, compared to surface irrigation with an average IE of 0.6 (van der Kooij et al., 2013; Abd El-Wahed et al., 2016; Grafton et al., 2018; Li et al., 2020). The concept of IE, defined as the ratio of irrigation water consumption (IWC) to irrigation water withdrawal (IWW), stems from irrigation engineering and is intended to inform the design of irrigation infrastructure (Van Halsema and Vincent, 2012). However, increasing IE does not necessarily increase the water availability (WA) at a watershed and basin scale due to the paradox of IE (Contor and Taylor, 2013; FAO, 2017; Ilyas et al., 2021). The paradox of IE can be considered as a special kind of Jevons Paradox (Alcott, 2005). The paradox of IE refers to the phenomenon that after increasing IE, IWC does not decrease as expected but increases. An important cause of the paradox of IE is that increasing IE may encourage farmers to expand the irrigation area (IA) or plant more water-intensive crops for economic benefits with the remaining water, thus increasing total water consumption by irrigation (Grafton et al., 2018). The phenomenon of the paradox of IE has been recognized in many regions globally (Huang et al., 2017; Lankford et al., 2020). For example, in Rajasthan, India, while using drip irrigation has increased IE, it has also increased the IA and the amount of water used for irrigation (Birkenholtz, 2017). Scott et al. (2014) also found that increasing IE has led to an increase in IA and water use in central Chile, southwestern United States, and south-central Spain. A recent study Zhang et al. (2022b) on Chinese Mainland also found that IE and IWC showed a strong positive correlation, and IWC increased significantly with the increase of IE. Because of this growing insight from numerous cases, it is also necessary to consider that increasing IE may lead to an increase in IWC (The paradox of IE).

Although studies have revealed the significant impact of human water use on hydrological drought, there is still much to understand about how investment in technologies to improve IE impacts hydrological drought in space and time. The catchment above Bengbu in the Huaihe River Basin (HRB) is chosen as the study area because it was frequently struck by drought disasters, and its hydrological process is strongly affected by human interventions, especially irrigation water use (Cheng et al., 2021). The overarching scientific questions we aim to address are the following: (1) How does irrigation water use change in the basin under the increase of IE (and IA) in an irrigation system? (2) What impact will the increase of IE (and IA) have on hydrological drought? Due to the unclear understanding of the above problems, the effectiveness of drought management measures is significantly compromised. Therefore, the purpose of this study is to reveal the impact of increasing IE on hydrological droughts so as to support drought management and water management decision-making regarding the implementation of irrigation policies. The structure of this paper is organized as follows: Section 2 of the paper introduces the study area. Section 3 describes the details of data and the methodology used in this study. The results and discussions are presented in Section 4. Lastly, conclusions are briefly drawn in Section 5.

2. Study area

2.1. The catchment above Bengbu in Huaihe River basin

The catchment above Bengbu in the Huaihe River Basin (CAB-HRB) is located in central eastern China, with a drainage area of about 121,300 km^2. The study area spans three provinces (Anhui, Henan, and Hubei Province) and 21 cities, with the Yellow River flowing along the northern border of the catchment (Fig. 1). The study area consists of mountains in the west part and plains in the middle and east parts. The area is dominated by the Asian monsoon climate, with annual average precipitation varying from about 600 mm/y in its northwest to about 1400 mm/y in its southern mountains. The study area has high agricultural water use, with arable land accounting for about 70 % of the total area. The main crop types in the northern parts of the study area are wheat and maize, while in the southern region rice is also planted, next to wheat and maize. Northern parts of the basin (mostly Henan Province, Fig. 1) are comparatively dry and have several large cities with large irrigation regions. The main irrigation methods used in the study area are surface irrigation, such as furrow irrigation and border irrigation, and also more efficient irrigation methods, such as drip irrigation. In addition, droughts occurred frequently in the HRB. The cumulative area suffered by drought was about 1.7×10^8 hm^2, and the grain loss was about 13.96×10^8 kg from 1949 to 2010 (Chen et al., 2013). In the summer of 2014, a severe drought occurred in the main tributary of HRB, i.e., the Shaying River (Schilstra et al., 2024), which seriously threatened the water supply of more than 1 million people. Another major drought occurred in 2019, which caused mainstream to break down, and 1110 ha of crops were affected, and 7×10^4 people had difficulty drinking water.

2.2. The change of IE and IA in the study area

Large parts of China are facing severe water scarcity, so it has implemented water-saving plans to conserve water resources at the national and local levels, such as the national long-term water-saving strategic plan (2001–2010), water-saving society plan (2011–2015, 2016–2020), and water-saving action plan (2019–2035) (Zhou et al., 2020). Water-saving irrigation has developed rapidly since 2000 (Huang et al., 2017). In 2009, the national water-saving irrigation plan, issued by the General Office of the State Council of China, required that the area with water-saving irrigation should make up to 80 % of the country’s effective IA by 2020. In addition, China’s Ministry of Water Resources has begun to calculate and report IE for each province annually since 2009. In 2011, the Chinese government set the goal of increasing IE to 0.55 by 2020, aiming to reduce water use for irrigation.

The IE improvement policy and its measures in China are implemented and supervised at the administrative district level. Therefore, for illustrative purposes, Henan Province, which occupies the largest area in our study area (Fig. 1), was chosen as an example. From 2000 to 2019, Henan Province implemented the water-saving society construction

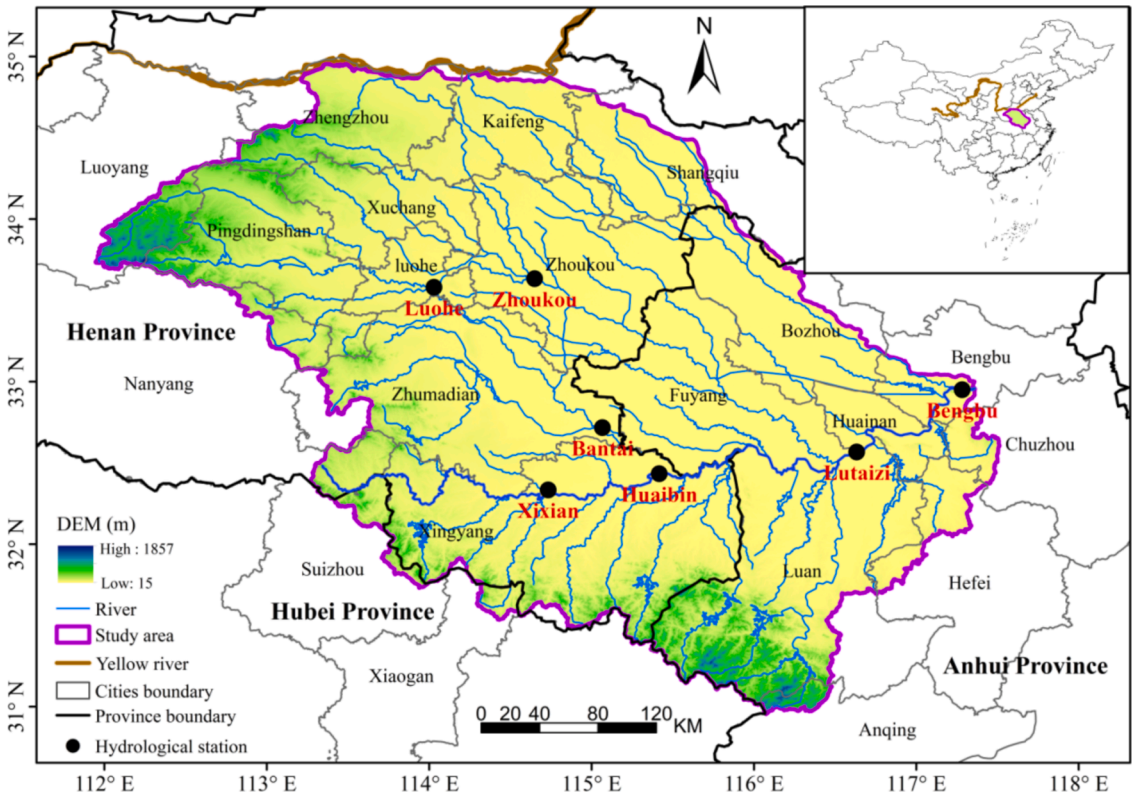

Fig. 1. Geographical location of the catchment above Bengbu in the HRB (CAB-HRB) and spatial distribution of provinces, cities, and hydrological stations.

plans of the "10th Five-Year Plan", "11th Five-Year Plan", "12th Five-Year Plan", and "13th Five-Year Plan". With the implementation of these plans, by 2010, the IE reached 0.570, and the IA under water-saving irrigation (e.g., sprinkler, micro, and pipe irrigation) reached 1537 × 10^3 ha. By 2015, the IA of the water-saving irrigation expanded to 1672 × 10^3 ha, and the IE increased to 0.601. By 2019, the IA of the water-saving irrigation increased to 2190 × 10^3 ha, with the IE reaching 0.615. In addition, measures such as water supply and use management, optimized water distribution technology, and canal system transformation have also been adopted in irrigated areas to increase IE.

Due to the data availability of IE, the illustration of the change of historical IE and IA in the study area was conducted at the provincial level from 2009 to 2019. Fig. 2(a) shows the variation of year IE and its trend estimated using the linear regression. The result shows that IE presented statistically significant increasing trends from 2009 to 2019, with about 0.005, 0.006, and 0.005 year^{-1} ($P < 0.05$) in Henan, Anhui, and Hubei, respectively. In terms of the growth rate of IE, Henan increased from 0.562 in 2009 to 0.601 in 2019, with an increase of 9 %; Anhui increased from 0.482 in 2009 to 0.544 in 2019, with an increase of 13 %; Hubei increased from 0.464 in 2009 to 0.522 in 2019, with an increase of 13 %. Fig. 2(b) displays the variation of year IA and its trend. It is worth noting that the IA of each province in the study area refers to the total effective IA of each city in the province involved in the basin (refer to Fig. 1). As such, IA in Henan is the largest, while Hubei IA is the smallest. The results also demonstrate a statistically significant increasing pattern for IA, with yearly increments of 36, 110, and 12 × 10^3 ha ($P < 0.05$) in Henan, Anhui, and Hubei, respectively.

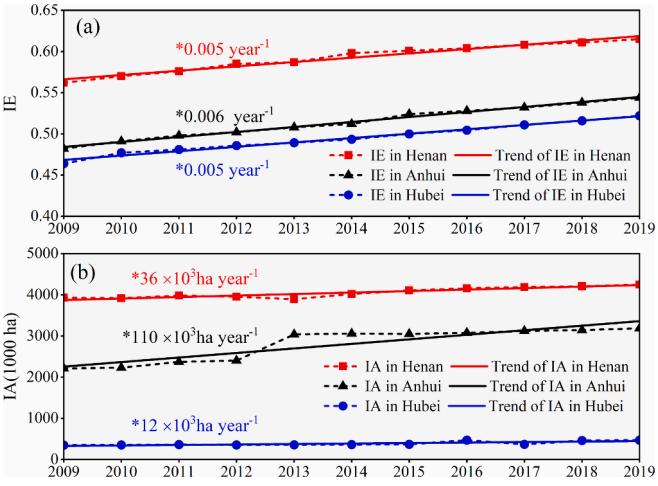

Fig. 2. (a) Variations of IE and IA in Henan, Anhui, and Hubei provinces within the study area along with their linear trends (* denotes $P < 0.05$) from 2009 to 2019.

3. Data and methods

3.1. PCR-GLOBWB 2.0 model

The global-scale hydrological model PCR-GLOBWB 2.0 model (Sutanudjaja et al., 2018) is adopted in the present study to simulate hydrological fluxes and storages in soil and groundwater, and to assess the effects of different irrigation practices on hydrological drought. The model is a physically based hydrologic and water resources model running at a spatial resolution of 5 arcmin (approximately 10 km). The model dynamically calculates the water storage and fluxes in two vertically stacked soil layers and an underlying groundwater layer for each grid cell at a daily time step. The model also simulates interactions between the topsoil layer and the atmosphere (snowmelt, evapotranspiration, and precipitation). Overland flow, subsurface flow, and groundwater baseflow are routed along the drainage network using a kinematic wave approach (de Graaf et al., 2014). The model integrates different human water uses (e.g., irrigation, domestic, and industry) and

solves the process of water withdrawal, consumption, and return flow of human water management (de Graaf et al., 2014). In this study, we considered industry, domestic, and irrigation water use. The gross and net industrial and domestic water demand are prescribed to the model (Sutanudjaja et al., 2018). The net irrigation water demand is calculated based on the crop composition and the IA per grid cell according to the FAO guidelines. After that, the gross irrigation water demand is estimated based on net irrigation water demand divided by IE (Döll and Siebert, 2002). In the PCR-GLOBWB 2.0 model, water withdrawal is set equal to gross water demand (summed over all the sectors) unless sufficient water is not available (Sutanudjaja et al., 2018). In case of insufficient WA, water withdrawal (surface water and groundwater) is scaled down to the WA, and then allocated proportionally to gross water demand per sector (irrigation, industry, and domestic) (Wada et al., 2014). Sector specific return flows of unconsumed abstracted water are included as well (de Graaf et al., 2014). In this study, IWC equals IWW multiplied by IE, while IWW multiplied by (1 − IE) equals the irrigation return flow (IRF). In the case of domestic and industry, their water consumption depends on the consumption coefficient (the ratio of net demand to gross demand) and equals water withdrawal multiplied by the consumption coefficient, while water withdrawal minus water consumption constitutes return flow.

The input parameters of the PCR-GLOBWB 2.0 model mainly include ten categories: meteorological forcing, land cover fraction, groundwater parameters, parameters related to phenology, ratio of cell maximum and minimum soil water storage to total soil water storage capacities, Arno scheme exponents defining distribution of soil water capacity, root fractions per soil layer, topographical parameters, upper and lower soil store parameters, and others including non-irrigation water demand, lakes and reservoirs, and desalinated water (Sutanudjaja et al., 2018). The output of the PCR-GLOBWB 2.0 model can be defined in the model according to the user's needs, mainly including the following categories (non-exhaustive): hydrological fluxes, such as discharge, baseflow, and interflow; human water management fluxes, such as water withdrawal (e.g., surface, groundwater, irrigation), water consumption (e.g., irrigation), and return flow (e.g., irrigation), and other fluxes, such as groundwater storage, interception storage, and soil water storage. More details about the model setup, structure, input parameters, output fluxes, and parameterization are given in previous publications (van Beek et al., 2011; Wada et al., 2014; de Graaf et al., 2014, 2019; Sutanudjaja et al., 2018).

We run the model at a 5 arcmin spatial resolution over the domain of CAB-HRB (Fig. 1, 121,300 km^2; 1836 grid cells in total) for the period 1979–2019. The model is forced by daily temperature and precipitation during 1979–2018 retrieved from the China meteorological forcing dataset (CMFD) (He et al., 2020, https://data.tpdc.ac.cn/zh-hans/) and in 2019 retrieved from the China meteorological dataset (CMA, http://data.cma.cn/). These meteorological data were interpolated to 5 arcmin using the bilinear interpolation method. To obtain gridded industry water demand, the census-based industry water usage data and gridded night-time light data were used. The census-based industry water usage data from 1979 to 2019 in 21 cities (Fig. 1) were obtained from the National Long-term Water Use Dataset of China (NLWUD, Zhou et al., 2020) and Water Resources Bulletins of China (WRB, https://www.mwr.gov.cn/). The relative light intensity map data with 5 arcmin resolution was retrieved from the Prolonged Artificial Nighttime-light Dataset of China (Zhang et al., 2021). Regional census-based industry gross water demands of all cities were downscaled to per grid cell based on the distribution of relative light intensity map (Droppers et al., 2020). Industrial water demands were kept constant in each month (Wada et al., 2014; Huang et al., 2018). For gridded gross domestic water demand, the census-based data retrieved from NLWUD and WRB of all cities were downscaled to per grid cell based on the distribution of population, which was retrieved from WorldPop gridded population dataset (WorldPop, https://www.worldpop.org/). Gross domestic water demands were disaggregated to monthly scale according to monthly temperature using the method of Wada et al. (2014) and Huang et al. (2018). The monthly temperature was obtained from CMFD and CMA. The net industry and domestic water demand were estimated by multiplying the gross demand with corresponding consumption coefficient, which was obtained from WRB.

Annual statistics of the IA in 21 cities (Fig. 1) and three provinces (Fig. 1, Henan, Anhui, and Hubei province) were retrieved from NLWUD and statistical yearbooks of three provinces. The statistical yearbooks of three provinces, which include the effective IA of each city of the study area (Fig. 1), were downloaded from the website of the China Statistical Information Network (http://www.tjcn.org/). The census-based IA were downscaled to the 5 arcmin grid scale following the method proposed by Wada et al. (2014) using the distribution of the gridded global map of IA, which was obtained from AQUASTAT dataset (https://www.fao.org/aquastat/zh/geospatial-information/global-maps-irrigated-areas). Data about IE in each province from 2009 to 2019 in the study area were collected from the Irrigation and Drainage Development Center of China (http://www.jsgg.com.cn/Index/Index.asp) and then were interpolated to the 5 arcmin gridded data uniformly. As no data is available for the period 1979–2008, values in 2009 are used for that period. Other data needed to parameterize the model, including soil parameters, groundwater parameters, and topographical parameters, were taken from the original global-scale model parameterization of the PCR-GLOBWB 2.0 model.

3.2. Model calibration and validation

We used the method proposed by Sutanudjaja et al. (2014), López López et al. (2017), and Ruijsch et al. (2021) to calibrate the PCR-GLOBWB model. As shown in Table 1, model parameters, including baseflow recession coefficient, soil saturated hydraulic conductivities, minimum soil water capacity, reference potential evapotranspiration, Manning's n, and crop *KC*, were calibrated using spatially uniform pre-factors (Table 1) based on stepwise calibrated method, instead of adjusting actual parameter values. The remaining parameters were kept unchanged.

The performance of discharge simulation was evaluated using the observed monthly discharge of 7 hydrological stations (Fig. 1) during the period 1981–2019, which was collected from the Bureau of Hydrology and Water Resources of Henan Province, China. The performance of water use simulation was evaluated using the reported yearly water withdrawal data from 1999 to 2019, which was collected from WRB of Huaihe River Basin (https://www.hrc.gov.cn/main/zfxxgkml/index.jhtml?channel_id=48). The simulation series of 1979–2019 was divided into three periods. The 1979–1980 was the spin-up period, the 1981–1999 was the calibration period, and the remaining of 2000–2019 was the validation period. Notably, as there was no reported water use data for the period of 1981–1998, the simulation of human water use was not calibrated.

Table 1
Six parameters, pre-factors, and adjustment functions used for calibrating the PCR-GLOBWB 2.0 model.

Parameters	Symbol	Pre-factors	Adjustment functions
Minimum soil water capacity	W_{min}	$f_w \in [0.5, 1.5]$	$W_{\min} = f_w \times W_{\min,ori}$
soil saturated hydraulic conductivities	K_{sat}	$f_k \in [-0.5, 0.5]$	$\log(K_{sat}) = f_k + \log(K_{sat,ori})$
Baseflow recession coefficient	J	$f_J \in [-0.5, 0.5]$	$\log(J) = f_J + \log(J_{ori})$
Reference potential evapotranspiration	$E_{p,0}$	$f_e \in [0.5, 1.5]$	$E_{p,0} = f_e \times E_{p,0,ori}$
Crop *KC*	KC	$f_{kc} \in [0.5, 1.5]$	$KC = f_{kc} \times KC_{ori}$
Manning's n	n	$f_n \in [0.5, 1.5]$	$n = f_n \times n_{ori}$

Note: The subscript "ori" denotes the parameters are original parameters.

The Nash-Sutcliffe coefficient of efficiency (*NSE*), correlation coefficient (*r*), and bias error (*Bias*, %) were used as the metrics to evaluate the performance of discharge simulation. The root mean square error (*RMSE*) besides *r* and *Bias* was used as the metric to evaluate the performance of water withdrawal simulation. The *r*, *NSE*, *Bias*, and *RMSE* are calculated as follows:

$$r = \sum_{t=1}^{T}(x(t)-\bar{x})(y(t)-\bar{y}) \Big/ \sqrt{\sum_{t=1}^{T}(x(t)-\bar{x})^2}\sqrt{\sum_{t=1}^{T}(y(t)-\bar{y})^2} \quad (1)$$

$$NSE = 1 - \sum_{t=1}^{T}[x(t)-y(t)]^2 \Big/ \sum_{t=1}^{T}[x(t)-\bar{y}]^2 \quad (2)$$

$$Bias = \left(\sum_{t=1}^{T}(x(t)-y(t) \Big/ \sum_{t=1}^{T}y(t)\right) \times 100\% \quad (3)$$

$$RMSE = \sqrt{\sum_{i=1}^{T}(x(t)-y(t))^2 / T} \quad (4)$$

Here, $x(t)$ and $y(t)$ denote observed discharge (reported water withdrawal) and simulated discharge (water withdrawal), respectively; t is the time step; T is the total time steps.

3.3. Scenario design

Increasing IE has long been hailed as an effective strategy to reduce water shortage. Paradoxically, despite the widespread application and gradual improvement of water-saving technologies, crop water consumption has increased in many countries (Perry et al., 2017). The paradox of IE refers to the phenomenon that the application of water-saving technologies does not reduce water consumption for irrigation but instead causes an increase in water consumption (Grafton et al., 2018). In general, the paradox of IE is the result of the interaction of hydrological, economic, social, institutional, and management factors. In our study area, the IE presented a steady increase from 2009 to 2019 (Fig. 2(a)). Therefore, we set up an IE increase alone scenario S1, in which IE increased as observed during the period 2009–2019. Notably, S1 is used to reveal the impact of increasing IE alone on hydrological drought, so in this scenario IA remains unchanged.

In addition to the fact that increasing IE (without changing the IA) may lead to the paradox of IE, another cause of the paradox of IE is that increasing IE may encourage farmers to plant more crops or more water-intensive crops, and consequently lead to an increase in water consumption by irrigation (Grafton et al., 2018; Xiong et al., 2021). As shown in Fig. 2(b), the IA in our study basin also increased significantly from 2009 to 2019. We further analyzed the relationship between IE and IA by extracting data from Fig. 2, as illustrated in Fig. 3. The results show a linear correlation between the increase of IA and IE. However, this relationship is not very strong. In fact, the increase of AI is influenced by many factors, such as the growing demand for food, the development of irrigation facilities, and the increase of IE (Sese-Minguez et al., 2017; Perry et al., 2017). Meanwhile, a recent study by Zhang et al. (2022a) in mainland China showed that the increase of IE contributes to about 22.2 % expansion of IA, particularly in water-scarce regions (31.5 %) compared to water-abundant regions (19.7 %). Therefore, to account for the potential impact of increasing IE leading to an increase in growing more water-intensive crops or more crops, we introduced a scenario S2, which assumes that both IE and IA increase, with IE increasing based on observed values. Considering the operability of scenario parameterization in the PCR-GLOBWB 2.0 model, we used the increase in IA in the model to consider the increase of more crops or more water-intensive crops in S2. It's challenging to determine the extent to which the increase in IA is solely due to the increase in IE, so we assumed that IA increases proportionally with the increase in IE from 2009 to 2019. The three scenarios are listed in Table 2.

The effect of IE increases alone (S1) and IE & IA increase simultaneously (S2) on the characteristics of hydrological drought in comparison with S0 were calculated as follows:

$$I_i = \frac{HD_{Si} - HD_{S0}}{HD_{S0}} \times 100\%, i = 1, 2 \quad (5)$$

Here, I_i is the percentage impacts of increasing IE alone (I_1) or increasing IE and IA (I_2) on hydrological drought characteristics; *HD* with different subscripts denotes drought characteristics in different scenarios.

3.4. Hydrological drought characteristics

A discharge threshold with a probability of exceedance between 70 ~ 90 % is commonly used in previous studies to identify the drought state (e.g., Wada et al., 2013; Cheng et al., 2021). In this study, the monthly streamflow with the exceedance probability of 80 % (Q_{80}) was selected as the threshold level, which was retrieved from the simulated discharge in S0. The drought state in a given month t at a grid cell (n) can be identified by:

Table 2
Scenario design and description in this study.

Scenario	IE	IA	Description
S0	The IE is fixed as the value in 2009	The IA is fixed as the value in 2009	Baseline scenario
S1	The IE increases as the actual values during 2009–2019.	The IA is fixed as the value in 2009	The situation of IE increases alone
S2	The IE increases as the actual values during 2009–2019.	The IA increases in proportion to the increase of IE in 2009–2019	Assumes that the increase of IE leads to an increase in more water-intensive crops or more crops

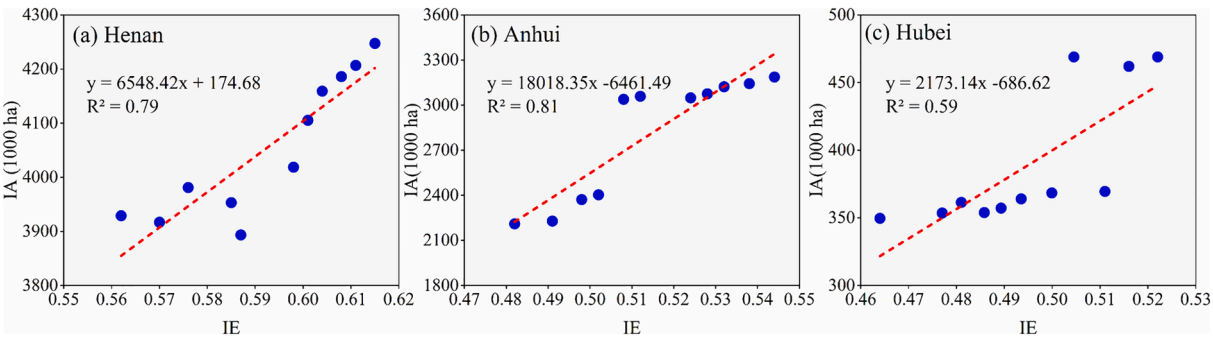

Fig. 3. Relationship between IE and IA of Henan, Anhui, and Hubei in the study area from 2009 to 2019.

$$S(t,n) = \begin{cases} 1, & Q(t,n) < Q_{80}(t,n) \\ 0, & Q(t,n) \geqslant Q_{80}(t,n) \end{cases} \quad (6)$$

where, $Q(t, n)$ is the monthly discharge of month t at grid cell (n); $Q_{80}(t, n)$ is the Q_{80} of month t at grid cell (n) during the period 1981–2019. $S(t, n)$ is a binary variable of month t at grid cell (n), with the value 1 and 0 represent drought state and no drought state, respectively.

The standardized drought streamflow deficit for month t at grid cell (n) ($SDSD(t, n)$) is calculated by:

$$SDSD(t,n) = \frac{\max(Q_{80}(t,n) - Q(t,n),\ 0)}{Q_{80}(t,n)} \quad (7)$$

The drought duration for each drought event i at grid cell (n) ($DD(i, n)$) is calculated by:

$$DD_{i,n} = \sum_{t=S_i}^{E_i} S(t,n) \quad (8)$$

where, S_i (E_i) is the start (end) time for the drought event i.

In addition, the percentage of drought area over study area at a month t ($PDA(t)$) is defined by:

$$PDA(t) = \frac{\sum_{n=1}^{N} S(t,n)}{N} \quad (9)$$

where, N is total number of grid cells of study area. PDA ranges from 0 to 1, with 0 and 1 represent that no grid cell is in drought and all grid cells are in drought, respectively.

4. Result and discussions

4.1. Model evaluation

Fig. 4 presents the performance of monthly streamflow simulation at seven hydrological stations (Fig. 1) in the calibrated period 1981–1999 and validated period 2000–2019. The results show that the simulated streamflow generally fits well with the observed streamflow process. In addition, as shown in Fig. 4, the value of r in the calibration and validation period ranged between 0.87 to 0.94 and 0.84 to 0.92, the value of NSE ranged between 0.72 to 0.89 and 0.68 to 0.85, and the value of $Bias$ ranged between −10 % to 6 % and −5% to 6 %, respectively. Overall, the NSE varies from 0.68 to 0.89, and the $Bias$ ranges between −10 % to 6 %, which indicates that the calibrated PCR-GLOBWB 2.0 model can simulate the hydrological process in the study area well.

Fig. 5 shows the performance of different types of water withdrawal (industry, domestic, and irrigation) simulation from 1999 to 2019. The results show that the model simulation of different types of water withdrawals generally matches the actual process of different water withdrawals. For IWW simulation, the r was 0.62, $RMSE$ was 13.0 mm/y, and $Bias$ was −5%. For industry water withdrawal simulation, the r was 0.91, $RMSE$ was 4.0 mm/y, and $Bias$ was 8 %. For domestic water withdrawal simulation, the r was 0.85, $RMSE$ was 2.7 mm/y, and $Bias$ was 4 %. It can be found that the simulation accuracy of industrial and domestic water withdrawal is better than that of IWW. This is due to that domestic and industry water withdrawal are simulated based on their water demand which is prescribed to the model (Sutanudjaja et al., 2018), while irrigation water demand is simulated by the model, which is affected by precipitation, soil, IA, and other data, so the simulated accuracy of IWW is lower than that of domestic and industry water withdrawal. In general, the value of r is greater than 0.6, and the absolute value of $Bias$ is less than 10 % for the three types of water withdrawal simulation, which indicates that the PCR-GLOBWB 2.0 model can capture the actual process of industry, domestic, and irrigation water withdrawal of the study area well, and can be used in the simulation analysis.

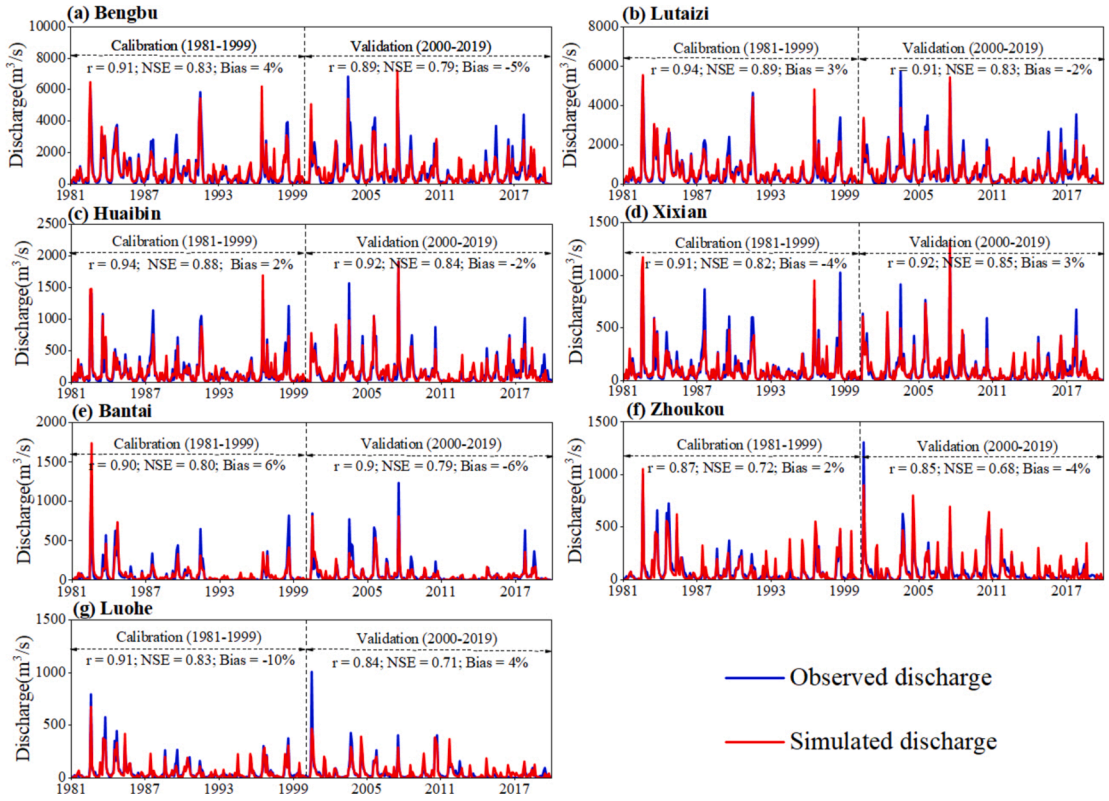

Fig. 4. Comparison of observed and simulated monthly streamflow at seven gauging stations ((a)~(g)) during the calibration period (1981–1999) and validation period (2000–2019).

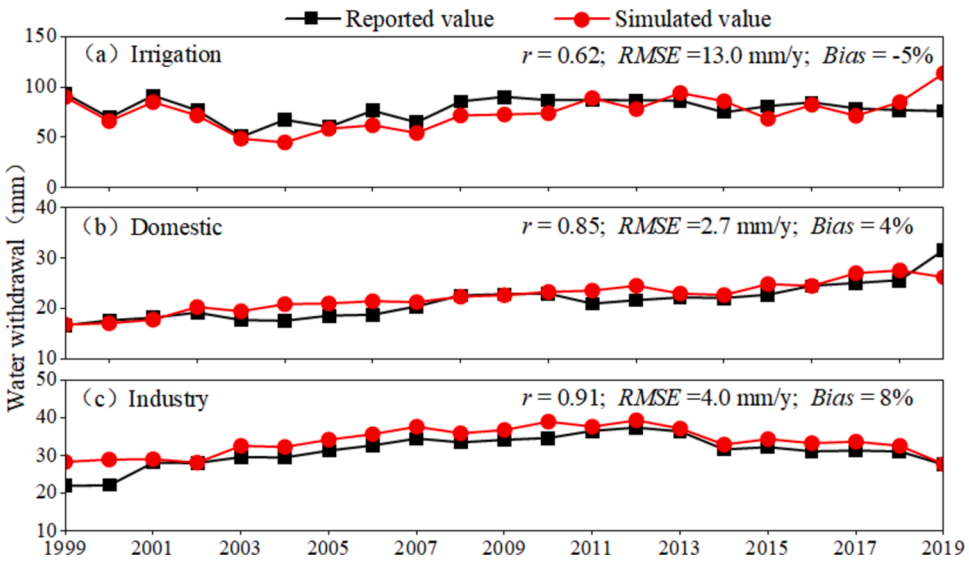

Fig. 5. Comparison of simulated and reported value of different types of year water withdrawal during the period of 1999–2019.

4.2. Impact of increasing IE on water use and water abstraction

Fig. 6 compares the yearly average IWW, IWC, and IRF over the study area from 2010 to 2019 under different simulated scenarios (S0, S1, and S2). The results clearly show that the impacts of increasing IE alone (S1) and increasing IE & IA simultaneously (S2) on irrigation water use are different. Compared with S0, the IWW in S1 decreases, while the IWW in S2 increases (Fig. 6(a)). In addition, the IWC in S1 is slightly higher than that in S0, while the IWC in S2 is the highest (Fig. 6(b)). The change of IRF and IWC caused by increasing IE exhibits different patterns. The IRF in S1 decreases compared with S0, while the IRF in S2 increases (Fig. 6 (c)). Those results indicate that increasing IE alone (S1) causes a decrease in IWW in the study area. However, IWC has increased, and accordingly, IRF has decreased. This is likely due to the relatively low WA in our study basin. When WA is low, increasing IE leads to an increase in water consumption. An expanded analysis of how increasing IE changes IWW, IWC, and IRF is discussed further in Section 4.4. In addition, when IE and IA both increased (S2), IWW, IWC, and IRF all increased. Meanwhile, it can be found that the increase in IWW and IWC of S2 is significantly higher than that of S1, which is due to the increase in IA leading to an increase in irrigation water demand.

Fig. 7 compares the simulated yearly surface water abstraction (SWA) and groundwater abstraction (GWA) of the study area from 2010 to 2019 under different scenarios (S0, S1, and S2). It is worth noting that the sum of SWA and GWA (Fig. 7) is significantly higher than IWW (Fig. 6(a)) because surface water and groundwater abstractions are not only used for irrigation water use but also for domestic and industry water use. The results clearly show that increasing IE alone and simultaneously increasing IE and IA have markedly different impacts on SWA and GWA. Compared with S0, the SWA in S1 decreases, while the SWA in S2 increases. In addition, the GWA in S1 is slightly lower than that in S0, while the GWA in S2 is significantly higher than that in S0. The

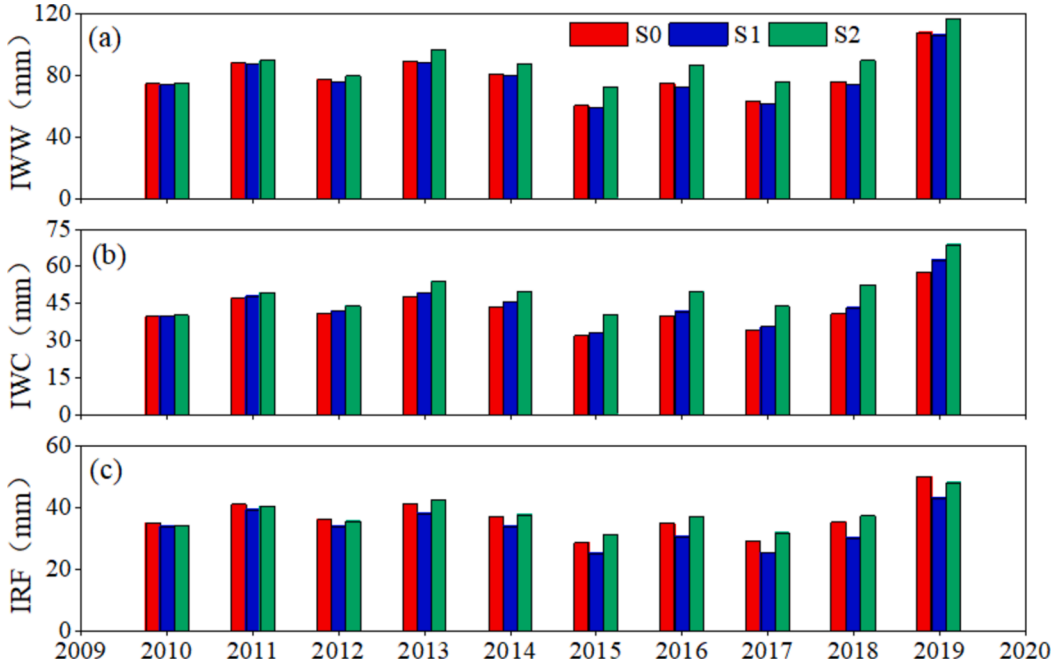

Fig. 6. Variation of (a) annual IWW, (b) IWC, and (c) IRF of the study area from 2010 to 2019 under different simulated scenarios.

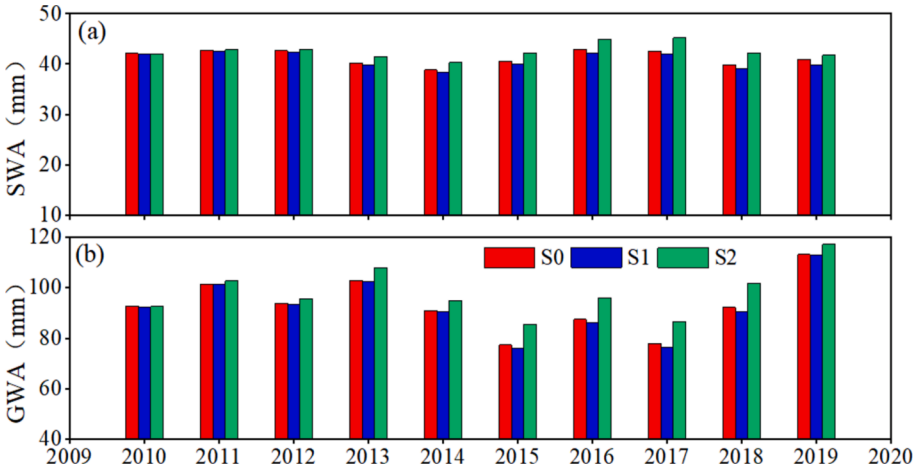

Fig. 7. Variation of (a) annual SWA (surface water abstraction) and (b) GWA (groundwater abstraction) of the study area from 2010 to 2019 under different simulated scenarios.

results demonstrate that the increasing IE from 2009 to 2019 resulted in a decrease in both SWA and GWA. However, when IE and IA increase simultaneously (S2), both SWA and GWA increase, and the increase of GWA is even higher than the increase of SWA. This change in GWA due to the simultaneous increases of IE and IA (in S2) is consistent with the results of Molle and Tanouti's (2017), which also showed that the use of advanced drip irrigation techniques has increased groundwater extraction in Morocco. Also, McVeigh and Wyllie (2018) found that in Snake River, Idaho, after farmers have increased IE, groundwater recharge reduced, and the Eastern Snake Plain Aquifer declined by about 30 % since the mid-1970 s, albeit precipitation increased.

4.3. Impact of increasing IE on hydrological drought characteristics

Fig. 8 presents the comparison of monthly standardized drought streamflow deficit (SDSD) volume and percentage of drought area (PDA) of the entire basin in different scenarios (S0, S1, and S2) from 2010 to 2019. SDSD volume and PDA in different scenarios (S0, S1, and S2) exhibit similar patterns of variation generally, especially in S0 and S1. Comparing the PDA and SDSD volume in S1 with those in S0, it can be seen that the drought characteristics in S0 and S1 do not differ much generally. There are cases where the SDSD volume in S0 is slightly larger than that in S1, such as in April 2014 when the SDSD volume in S0 is about 20.4 while in S1 is about 17.8. Meanwhile, there are also cases where the SDSD volume in S1 is larger than that in S0, for example, in July 2014 when the SDSD volume in S0 is about 886.7 while in S1 is about 899.4. However, the SDSD volume and PDA under the S2 are larger than those in S1 and S0, and the increase after 2015 is significantly higher than that before 2015, which indicates that increasing IE and IA simultaneously (S2) significantly increases the hydrological drought, and the higher the increase in IE (resulting in the higher the increase in IA), the greater the aggravated impact on hydrological drought. In addition, it can be detected that the gap between drought characteristics (e.g., PDA) in S2 and S0 in drought months (high PDA) is significantly higher than that in non-drought months (very low PDA). This indicates that the impact of increasing IE and IA on hydrological drought is more significant during drought, mainly due to low WA combined with high irrigation demand when drought happens. However, for extreme drought, such as July 2014 and June 2019 (two months with the highest SDSD and PDA), the gap between drought characteristics (e.g., PDA) in S2 and S0 is relatively small. This is because human activities have limited influence on extreme droughts, where natural variability becomes the predominant factor (Stott, 2016). These finding indicates that the paradox of IE is more pronounced during droughts, but its impact diminishes during extreme droughts.

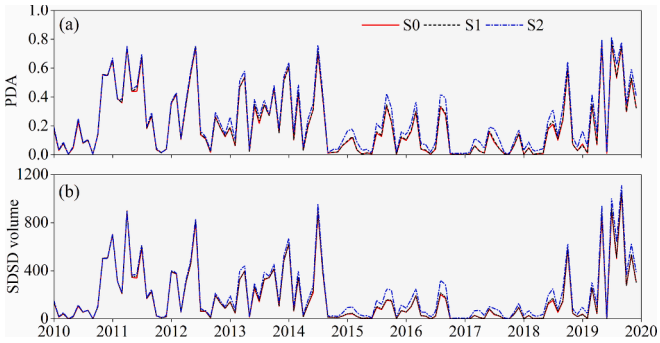

Fig. 8. Comparison of the monthly *PDA* and *SDSD* volume over the entire basin for different scenarios from 2010 to 2019.

Fig. 9 illustrates the impacts of increasing IE alone (S1) and increasing both IE & IA (S2) on monthly PDA and SDSD over the entire study area from 2010 to 2019. It can be found that whether it is increasing IE alone (S1, Fig. 9(a)) or increasing IE & IA simultaneously (S2, Fig. 9(b)), there are situations where the impacts are greater than 0 and the impacts are less than 0, which indicates that the increase of IE and both increases of IE & IA have the dual roles of aggravating and alleviating hydrological drought. In addition, the mean and median values of the impact of increasing IE on PDA were 2.5 % (the green dot in Fig. 8) and 1.1 % (the black line in the box in Fig. 8), while the mean and median values of the impact of increasing IE & IA on PDA were 79.4 % and 21.0 %. Meanwhile, the mean and median of the impact of increasing IE on SDSD were 4.8 % and 1.3 %, while in the case where IE and IA both increase, the mean and median of the impact on SDSD were 188.8 % and 29.9 %. These results show that although increasing IE can both aggravate and alleviate the hydrological drought, the aggravating effect is dominant, especially in the case of IE and IA increasing simultaneously (S2); increasing IE & IA significantly aggravates hydrological drought in the basin as the increase in IA leads to the increase in IWC.

Fig. 10 shows the spatial impacts of increasing IE and increasing IE & IA on average DD and SDSD on the grid cell basis during the period of 2010–2019. In general, the spatial impact of increasing IE (and IA) on DD and SDSD also presents dual characteristics, i.e., alleviating hydrological drought in some grid cells while exacerbating it in others. Taking the impact of increasing IE on SDSD as an example (Fig. 10(c)), increasing IE alleviated SDSD in the central parts of the study area, and the corresponding contributions vary mainly in the range of −60 % ~ −5 %. However, in the northern edge of the study area, the SDSD was intensified, where the SDSD of some grid cells even increased by more

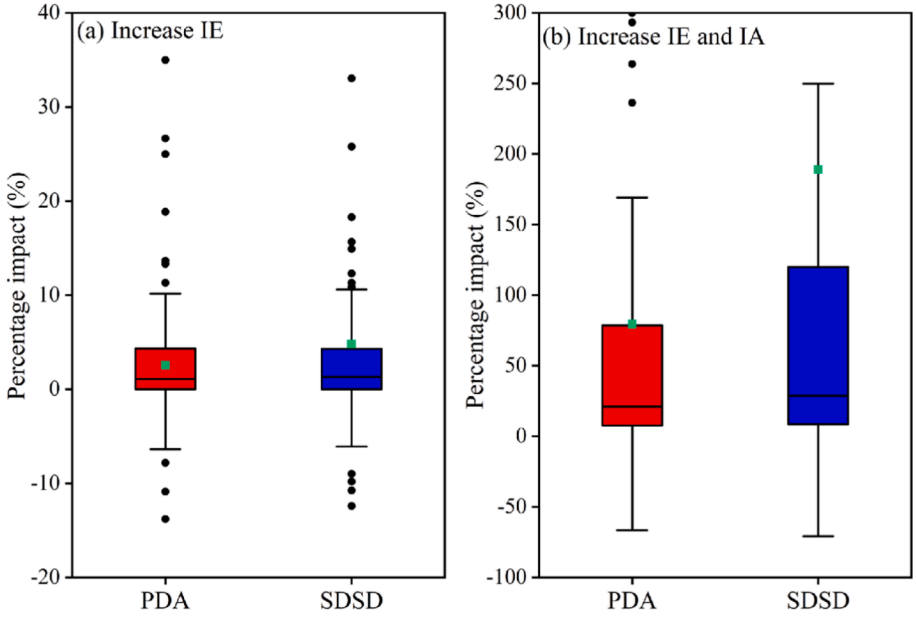

Fig. 9. Box plots of impacts of increasing IE and increasing IE & IA on monthly *PDA* and *SDSD* of total study area during the period of 2010–2019.

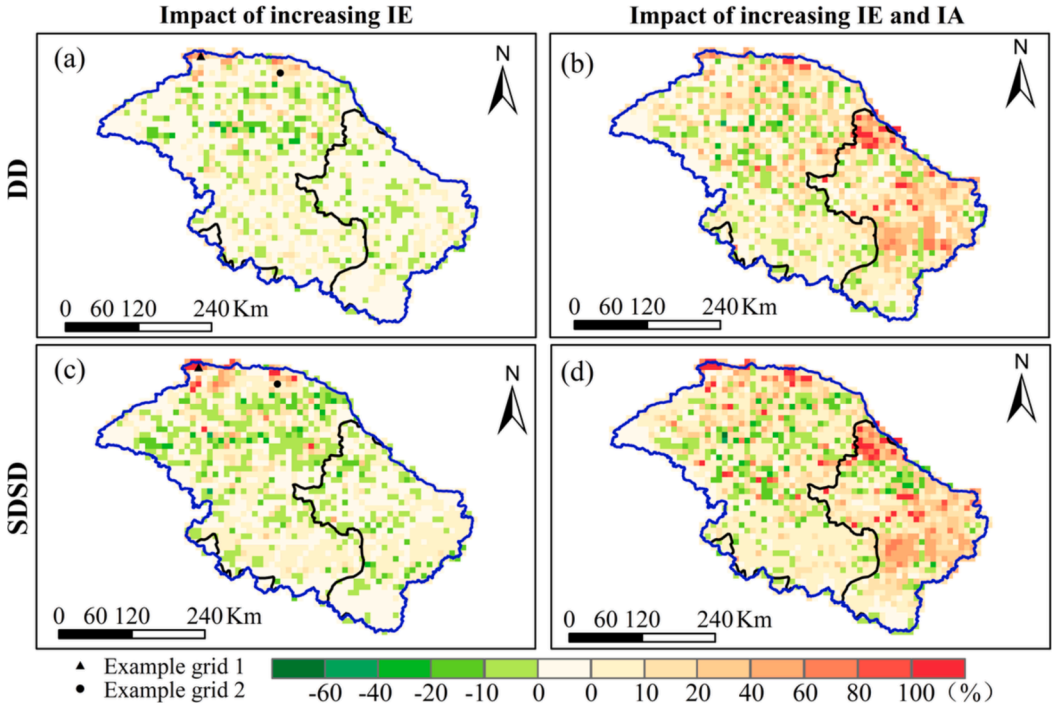

Fig. 10. The spatial pattern of the relative impacts of increasing IE and increasing IE & IA on the annual mean *DD* (drought duration) and *SDSD* during the period of 2010–2019.

than 80 %. As for the impact on SDSD under increasing both IE and IA (Fig. 10(d)), although it generally presents positive impacts (aggravating the hydrological drought), there are also places, such as the central region of the study area, where drought severity (SDSD) was reduced, mostly in the range of −40 % ∼ −5 %. The above results indicate that the impact of increasing IE on hydrological drought is complicated, that is, it exacerbates and alleviates hydrological drought simultaneously in time and space. In the Discussion Section (Sections 4.4.1 and 4.4.2), we will deeply discuss why increasing IE (and IA) have opposing roles in hydrological drought. In addition, the alleviation degree of increasing IE alone (S1) on DD and SDSD is higher than that of increasing both IE and IA (S2), while the intensified degree of increasing IE and IA on DD and SDSD is significantly higher than that of increasing IE alone, which is basically consistent with the results of the whole study area in Fig. 9, namely, increasing both IE and IA (S2) significantly intensifies hydrological drought.

4.4. Discussions

4.4.1. Why does increasing IE alone have two-sided effects on hydrological drought?

The purpose of increasing IE can be to reduce IWW, free up water for

other allocations, or reduce the use of surface water and groundwater (Lankford et al., 2020). For example, a study in Spain by Espinosa-Tasón et al. (2020) concluded that IWW decreased after implementing the intense efficiency improvement policy. In this way, increasing IE could supplement the river discharge to a certain extent, consequently alleviating the aggravating impact of irrigation on hydrological drought. However, our results show that increasing IE alone (S1) can both aggravate and alleviate hydrological drought in time and space. In this section, we discuss why does increasing IE have the opposing roles in hydrological drought by investigating whether increasing IE leads to the paradox of IE.

In this study, we used the water accounting method based on water balance to reveal the mechanism of increasing IE affecting hydrological drought. Here, we use an assumptive case to show how the increase of IE changes the irrigation water use (Fig. 11). In this case, assuming that the crop net water demand (NWD) of an irrigation system in an irrigation period is 100 mm, the IE is 0.5 (Scenario 1), and Scenario 2 uses advanced irrigation technology to increase IE, which is assumed to increase to 0.8. From Scenario 1 to 2, only IE increases, IA does not increase, and there is no switch to more water-intensive crops. Therefore, the NWD is still 100 mm after increasing IE to 0.8 in Scenario 2. However, from Scenario 1 to 2, the crop gross water demand (GWD) decreases from 200 mm to 125 mm. As shown in Fig. 11, increasing IE may lead to three consequences under the influence of WA: ① reduces IWW and IWC keeps unchanged; ② IWW keeps unchanged but increases IWC; ③ reduces IWW but increases IWC. For Consequence ①, it occurs when water resources are relatively abundant and can meet crop water requirements, corresponding to Situation I in Fig. 11. For Situation I, increasing IE leads to "Reducing the total amount of water used for irrigation"; For Consequence ②, it happens when water resources are comparatively dry with limited WA and cannot meet most of the crop water requirement, corresponding to Situation V in Fig. 11. At Situation V, after increasing IE, IWW does not decrease, but IWC increases. Therefore, increasing IE consumes more water instead, which indicates that increasing IE leads to the paradox of IE; For Consequence ③, according to the relative changes of IWW and IWC, it can be further divided into three situations, corresponding to Situation II, III, and IV in Fig. 11. For Situation II, the decrease of IWW is higher than the increase of IWC, which can "Reduce the total amount of water used in irrigation" after increasing IE. For Situation III, the decrease of IWW is equal to the increase of IWC, which keeps balance after increasing IE. For Situation IV, the decrease of IWW is less than the increase of IWC, which means that increasing IE leads to the paradox of IE.

The above five situations indicate that increasing IE may or may not lead to the paradox of IE depending on different WA (Fig. 11). We further compared these five situations with a comprehensive study by Lankford (2023), which identified and analyzed 20 scenarios (cases) of water conservation or paradox outcomes using the irrigated systems accounting model. Both studies indicate that in some situations, increasing IE can reduce water withdrawal. Interestingly, Lankford (2023) does not indicate a case where IWW remains unchanged after increasing IE in a situation of water scarcity (like Situation V in our study). This raises the question of whether this scenario can be found in actual irrigated areas. Berbel et al. (2015) do indicate such a case, where there is sufficient water, and IE increases and hence no paradox occurs (without IA expansion). Conversely, in a situation of water scarcity, the increase in IE leads to higher water consumption. In general, we enriched the insights into the paradox of IE by working out five situations. However, we realize that, in reality, a plurality of possible outcomes emerges as efficiency improvements go along with other developments in the locality. Lankford (2023) worked out more scenarios by analyzing 20 cases of water conservation. Nevertheless, the main (methodological) challenge remains in understanding and mapping actual field cases to complement our identified scenarios.

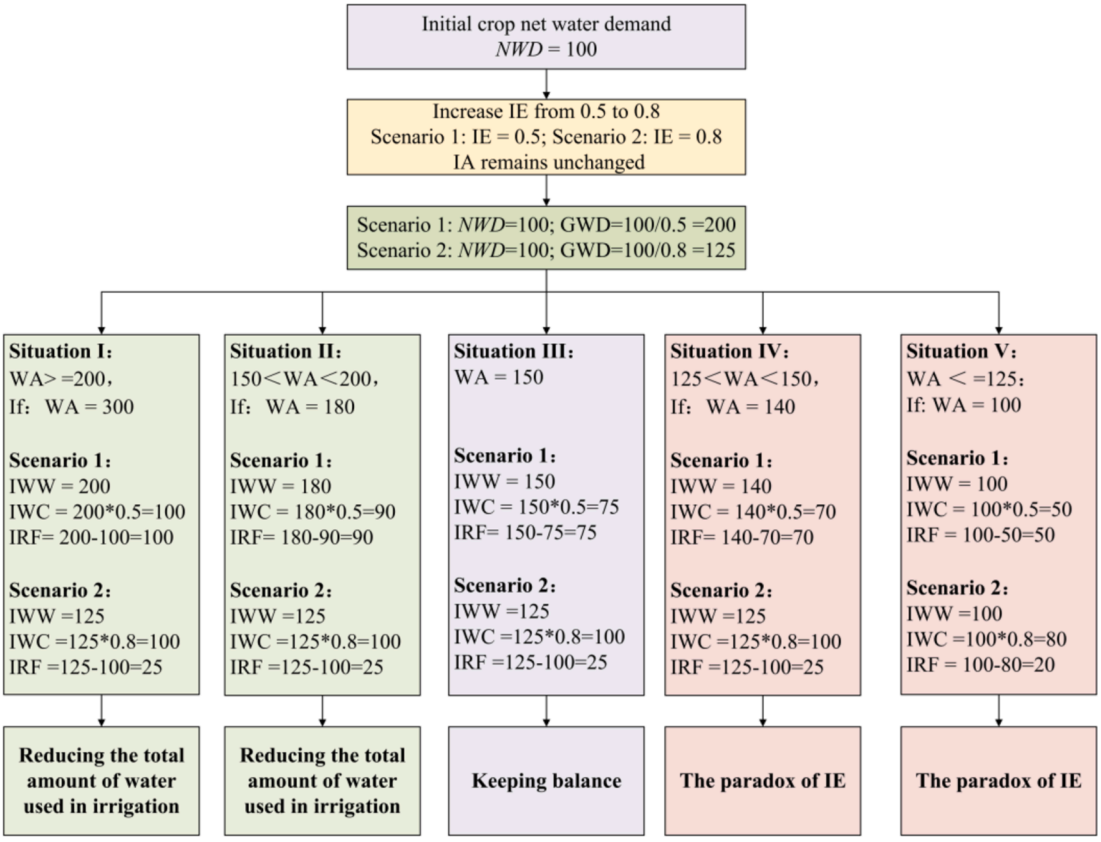

Fig. 11. A case of five possible situations leading to three consequences after increasing IE. Note: IE has no dimension, and the unit of other variables in the figure is mm.

Our results show that the increase of IE (S0 to S1) resulted in an average decrease of about 1 mm in IWW and an average increase of about 2 mm in IWC over the whole study area during 2010–2019 (Fig. 6), which belongs to paradoxical Situation IV in Fig. 11. The increase in IE led to a reduction in the amount of water withdrawn for irrigation (1 mm). However, it also resulted in more water being consumed by evapotranspiration (2 mm), ultimately reducing the water flow in the streams. As a result, the increase in IE caused higher values of SDSD and PDA. Therefore, the increase of IE slightly aggravated the hydrological drought in the study area. In addition, increasing IE can aggravate or alleviate drought at different times from the perspective of the whole study area, which is due to whether the irrigation water demand is met due to different WA at different times. When water resources are relatively abundant, increasing IE will lead to a situation (e.g., I or II in Fig. 11) in which the decrease of IWW is higher than the increase of IWC (or IWC does not increase). In this situation, increasing IE alleviates the hydrological drought as intended. However, when water resources are scarce with limited WA and cannot meet most of the crop water requirement, increasing IE will lead to a paradoxical situation (e.g., IV in Fig. 11) in which the increase of IWC is higher than the decrease of IWW (or IWW does not decrease). In this paradoxical situation, after increasing IE, the relative increase of water consumption and the relative decrease of return flow in the basin makes the hydrological drought intensify. The three possible consequences of increasing IE in this study also support why many studies revealed that most of the cases where increasing IE does not result in "water savings" are in relatively arid regions, such as Xinjiang (Liu and Tian, 2016) and Northeast China (Zhou et al., 2020), and Africa (Molle and Tanouti's, 2017). In these areas, the climate is dry, water resources are scarce, and irrigation usually cannot meet most of the crop water demand; increasing IE will make irrigation more "adequate", which thus increases IWC.

Although Fig. 11 can also explain the dual roles of increasing IE affecting hydrological drought in space, it cannot be used for some grid cells. For example, in the northern edge of the study area, increasing IE aggravated hydrological drought in some grid cells (Fig. 10(a) and (c)). In these grid cells, the water is imbalanced, and therefore, cannot use the water balance approach to water accounting. For these grid cells, we selected two example grid cells, as shown in Fig. 10(a) and (c). In Fig. 10 (a) and (c), the triangular and circular black dots are examples of grid cells 1 and 2, respectively. These two example grid cells had a 194 % (grid cell 1) and 71 % (grid cell 2) increase in SDSD after increasing IE (S1 VS S0). As shown in Fig. 12, the simulated discharge in S1 for these two grid cells shows an overall trend of less than S0, especially in drought periods. Table 3 exhibits the average total water withdrawal (TWW), non-irrigation water withdrawal (NWW), IWW, IWC, and IRF of two example grid cells for S1 and S0 during the period of 2010–2019. The results show that increasing IE led to a decrease in IWW and an increase in IWC in both grid cells, but the increase in IWC is smaller than the decrease in IWW (Table 3). Therefore, using Fig. 11 cannot explain why increasing IE exacerbated the hydrological drought in these two grid cells. However, in both two scenarios (S0 and S1), the sum of NWW and IWW is greater than the TWW of these two grid cells (Table 3), which indicates these two grid cells are comparatively water-scarce with limited WA locally and large requirements for human water use. To meet water demand, the model not only abstracted water from their own grid cells, but also took water from other adjacent grid cells. Therefore, the increase in IE led to a reduction in IWW, which means that the amount of water withdrawn from other adjacent grid cells (not local grid cells) is reduced. Thus, the increase in IE aggravated hydrological drought in those grid cells due to the decrease in the volume of "water transfer" from their adjacent grid cells.

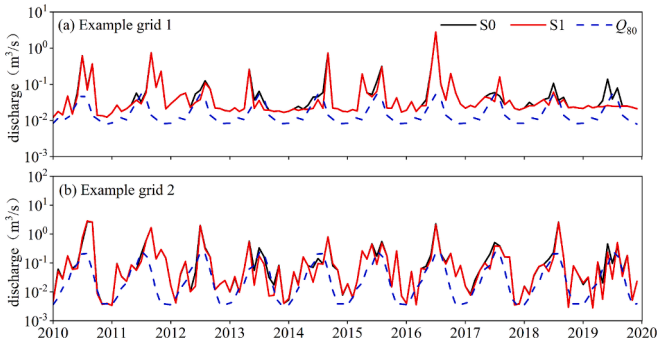

Fig. 12. Monthly discharge in S0 and S1, and the threshold level Q_{80} (derived from S0) on two example grid cells.

Table 3
Average TWW, NWW, IWW, IWC, and IRF of two example grid cells from 2010 to 2019 under S1 and S0.

Grid cells	Scenario	TWW (mm)	NWW (mm)	IWW (mm)	IWC (mm)	IRF (mm)
Example grid cell 1	S0	205.4	93.3	139.9	78.6	61.3
	S1	205.5	93.3	134.7	80.3	54.4
	Difference	0.1	0.0	−5.2	1.6	−6.9
Example grid cell 2	S0	56.0	56.9	243.5	136.9	106.7
	S1	53.7	56.9	233.6	139.4	94.2
	Difference	−3.3	0.0	−10.0	2.5	−12.5

Note: The difference is equal to the value in S1 minus the value in S0. *TWW* and *NWW* denote the total water withdrawal and non-irrigation water withdrawal, respectively.

In summary, increasing IE has different impacts (aggravation or alleviation) on hydrological drought under different WA. When water resources are relatively abundant, increasing IE will lead to a situation in which the decrease of IWW is higher than the increase of IWC. In this situation, increasing IE alleviates the hydrological drought as intended. However, when water resources are scarce with limited WA and cannot meet most of the crop water requirement, increasing IE will lead to the paradox of IE and consequently aggravate the hydrological drought. Also, increasing IE could aggravate the hydrological drought in water-receiving areas as it reduces water supply from outside regions.

4.4.2. Why does increasing both IE and IA have two-sided effects on hydrological drought?

The current understanding of an important cause of the paradox of IE is that increasing IE may encourage farmers to grow more crops or more water-intensive crops under government subsidies, thus increasing IWC and making it fall into a "water saving" dilemma (Xiong et al., 2021; Grafton et al., 2018). In this study, the behavior of farmers planting more crops or more water-intensive crops was considered by the increase of IA in the PCR-GLOBWB 2.0 model. Our results show that increasing IE and IA on hydrological drought also has two-sided effects in time and space, i.e., aggravating and alleviating hydrological drought, with the aggravating effect clearly dominant. In this section, we discuss why does increasing IE and IA have two-sided effects on hydrological drought by investigating whether increasing IE and IA leads to the paradox of IE.

Similar to Fig. 11, the water accounting method based on water balance is used to investigate the possible change of irrigation water use after increasing IE and IA, as shown in Fig. 13. In Fig. 13, there are two IE scenarios: Scenario 1 has an IE of 0.5, and Scenario 2 has an IE of 0.8. Notably, the NWD and GWD both increase due to the increase in IA from Scenario 1 to 2. When the increasing IE leads to the increase of IA, there are three possible consequences:① IA increases in a proportion smaller than the increase of IE; ② IA increases in proportion to the increase of IE; ③ IA increases in a proportion higher than the increase of IE. For both consequences ② and ③, once occurring, both result in the IWW of Scenario 2 is always greater than or equal to that of Scenario 1, and the IWC of Scenario 2 is always higher than that of Scenario 1. Therefore, consequences ② and ③ always lead to the paradox of IE. For

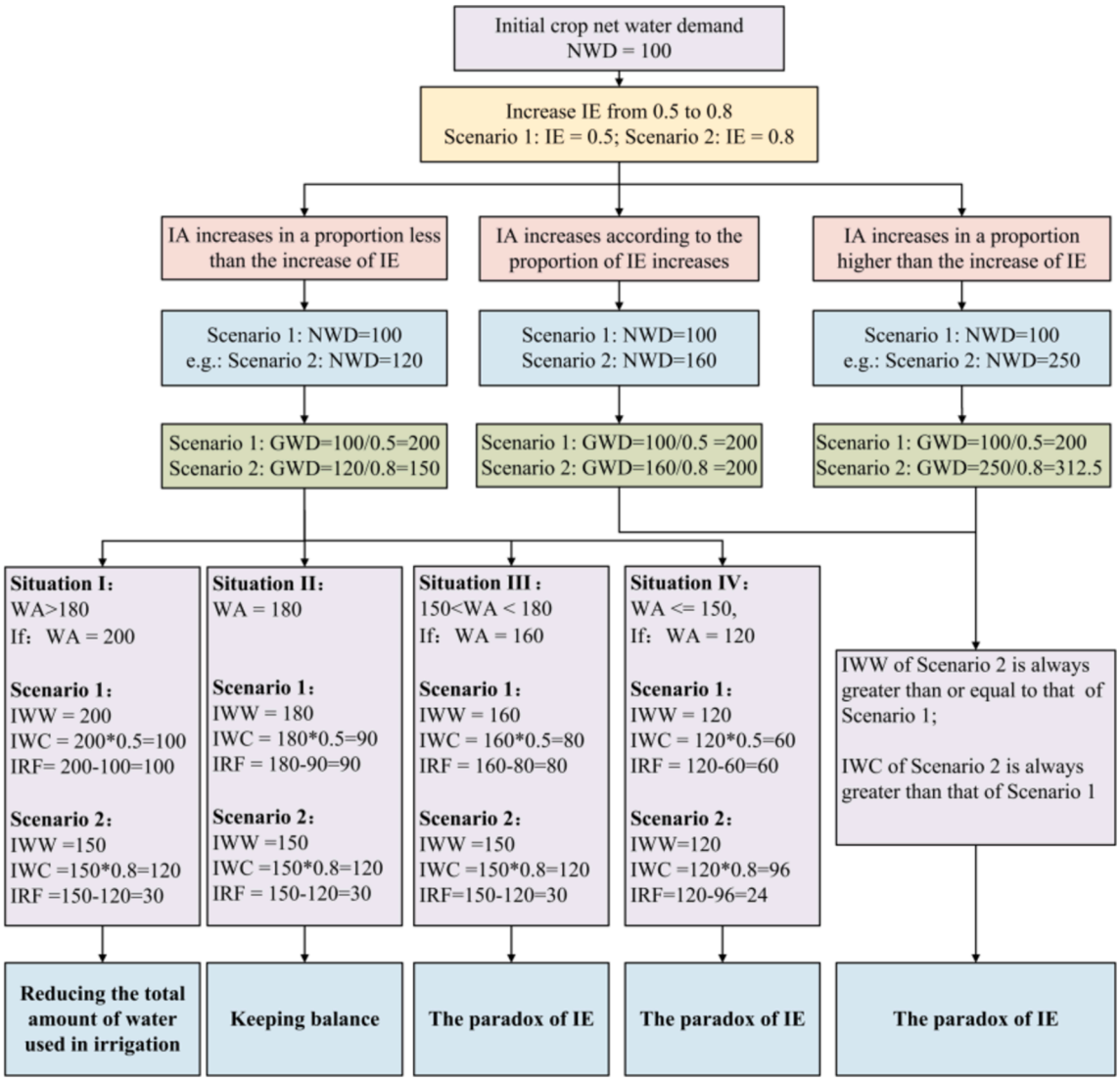

Fig. 13. A case of the possible consequences after increasing IA and IE. Note: IE has no dimension, and the unit of other variables in the figure is mm.

consequence ①, whether it leads to the paradox of IE is affected by WA. As shown in Fig. 13, increasing IE and IA may have four situations under the influence of WA. For Situation I, it occurs when water resources are relatively rich (high WA), and the GWD of two scenarios can be met. In Situation I, after increasing IE and IA, the IWW reduces while IWC increases, but the reduced amount of IWW (50 mm) is greater than the increased amount of IWC (20 mm). Therefore, in Situation I, increasing IE and IA reduces the total amount of water used in irrigation, indicating that increasing IE and IA does not lead to the paradox of IE; For Situation II, it happens when the water resources are relatively average. From Scenario 1 to 2, IWW decreases by 30 mm while IWC increases by 30 mm, i.e., the decrease in IWW and the increase in IWC are maintained in balance, meaning neither reducing water used in irrigation nor more water is consumed. For Situation III, it happens when the water resources are more average. In this situation, IWW decreases by 10 mm after increasing IE and IA. However, IWC increases by 40 mm, which indicates that increasing IE and IA leads to the paradox of IE, namely, increasing IE and IA consumes more water (30 mm). For Situation IV, it occurs when water resources are poor, and the WA is so small that the NWD and GWD cannot be met. In Situation IV, the IWW remains unchanged from Scenario 1 to 2. However, the IWC of Scenario 2 (96 mm) is significantly higher than that of Scenario 1(60 mm), which indicates that increasing IE and IA results in the paradox of IE.

The above situations indicate that increasing IE and IA results in an increase in IWC, regardless of whether the IWW decreases, increases, or remains unchanged (Fig. 13). Lankford (2023) demonstrated a case of IE-induced depletion and area rebound (Case 4). In this case, IE increased from 0.45 to 0.85, and the zone area expanded by 356 ha from the baseline of 400 ha. As a result, irrigation withdrawal overplus increased 197 hm^3, and total zone depletion increased 0.25 hm^3, aligning with consequences ② of this study (see Fig. 13). The reason for this lies in the similarity in the increase of IE and zone area in Case 4 of Lankford's study, both around 89 %. Compared to Lankford (2023), this study considered more cases of the increase in IA, that is, IA increases in a proportion smaller than, in proportion to, and a proportion higher than the increase of IE. More importantly, we analyzed and proposed more situation results of increasing IE and IA under different water shortage-related WA.

Our results show that increasing IE and IA significantly increased IWW by 8 mm and IWC by 7 mm (S2 VS S0) on average over the whole study basin during 2010–2019, see Fig. 6. Therefore, this result does not belong to consequence ①, which is due to the fact that IA increases in proportion to the increase of IE when designing the scenario (Table 2), and thus belongs to consequence ②. consequence ② always results in the paradox of IE, and therefore, it should always have positive impacts on hydrological drought. However, although the IA is set to increase in

proportion to the increase of IE, the increase of IA is also constrained by the irrigation system, for example, the size of the land area that can be cultivated in an irrigation system limits the expansion of IA. For the PCR-GLOBWB 2.0 model with a grid cell as the irrigation system, the IA cannot exceed the area of grid cell (Wada et al., 2014; Sutanudjaja et al., 2018). When the size of IA reaches the area of grid cell, it is not possible to expand the arable land. Fig. 14 exhibits the IA in S0 and S2 and its comparison in 2019. It can be found that the IA of some regions (e.g., the central part of the study area) is limited by the size of grid cell, and its growth rate does not increase according to the increase of IE, for example, the increase of IA in the central part of the study area mostly ranged between 2 ~ 4 % (S2 vs S0), less than the increase of IE (Fig. 3 (a)). At this time, the change of irrigation water use caused by increasing IE and IA belongs to the consequence ①(Fig. 13). For consequence ①, increasing IE and IA may result in "Reducing the total amount of water used in irrigation", "Keeping balance" or "The paradox of IE" under different WA situations. Therefore, under the combined effect of the changes of IA in consequences ① and ②, the increase of IE and IA has the dual effects of alleviating and aggravating hydrological drought, with the aggravating effect dominant. It is dominant for aggravating the hydrological drought because the increase in IA leads to an increase in irrigation water demand (NWD and GWD), thus leading to a significant increase in IWC and IWW. However, when the increase of IA is restricted by the irrigation system, the intensification effect of increasing IE and IA on hydrological drought will be weakened. Notably, when the IA cannot increase or only slightly, increasing IE and IA can result in a situation in which the decrease of IWW is greater than the increase of IWC (Situation I in Fig. 13). In this situation, increasing IE and IA alleviates the hydrological drought as intended.

In summary, despite increasing IE and IA having two-sided effects on hydrological drought, the aggravating effect is dominant due to the increase in IA leading to a significant increase in IWC and IWW. However, when the irrigation system restricts the increase of IA, the intensification effect of increasing IE and IA on hydrological drought will be weakened. Notably, when the IA cannot increase or only slightly, increasing IE and IA can result in the decrease of IWW being more significant than the increase of IWC and consequently alleviates hydrological drought (as intended).

4.4.3. *Limitations of the hydrological modeling in the study*

There are some limitations in our hydrological modeling for assessing the effects of increasing IE on the hydrological drought, which should be addressed in the future. Firstly, water withdrawal from groundwater and surface water in the PCR-GLOBWB 2.0 model is sector independent, which means that the available water resources are allocated proportionally to the amount of domestic, industry, and irrigation water demands, without considering possible local preferences (de Graaf et al., 2014). However, different sectors have their different water use priorities. Usually, domestic water demand has the highest priority, followed by industry, and finally irrigation. In addition, the competition of water uses in different sectors often happens in water-scarce places, particularly for surface water (Wada et al., 2014).

Secondly, the IWC is calculated based on transpiration, evaporation, and IWW in the PCR-GLOBWB 2.0 model, which enables the model dynamically to link the feedback between the irrigation water, the changes in surface and soil water, and evapotranspiration (Sutanudjaja et al., 2018). However, this calculation method may lead to a water imbalance in which IWW is not equal to IWC plus IRF. Therefore, we adjusted the calculation method in the model, that is, IWC equals IWW multiplied by IE, and IRF equals IWW multiplied by (1-IE). Our calculation method is consistent with another hydrological model CWatM v1.04 model (Burek et al., 2020). In addition, IE is a static value in the model, which cannot consider changes in IE caused by the development of irrigation technology (de Graaf et al., 2014; Sutanudjaja et al., 2018). In this study, we improved the model to consider dynamic IE using the time series of reported IE. However, due to data availability, IE is set as a uniform value for each province (see Fig. 2(a)), which ignores the spatial variability of IE due to different irrigation measures (Irmak et al., 2011). Meanwhile, the interannual variation of IE is ignored as only yearly value of IE is available.

Thirdly, in the PCR-GLOBWB 2.0 model, the irrigated water is lost through percolation and recharged to groundwater as IRF (Sutanudjaja et al., 2018). However, in the real world irrigation water losses not only infiltrate into groundwater but also occur in the process of water conveyance in the form of evaporation from canals, leaks in pipelines, and canal seepage (Van Halsema and Vincent, 2012; Irmak et al., 2011). Therefore, the amount of groundwater recharged by IRF is likely overestimated by the model. In general, the modeling could be improved by optimizing water allocation schemes that consider possible local preferences, collecting more detailed data about IE, and including water conveyance losses in the calculation for irrigation losses and IRF in the PCR-GLOBWB 2.0 model.

Finally, we used the increase in IA in the PCR-GLOBWB 2.0 model to represent the scenario (S2) where farmers grow more crops and more

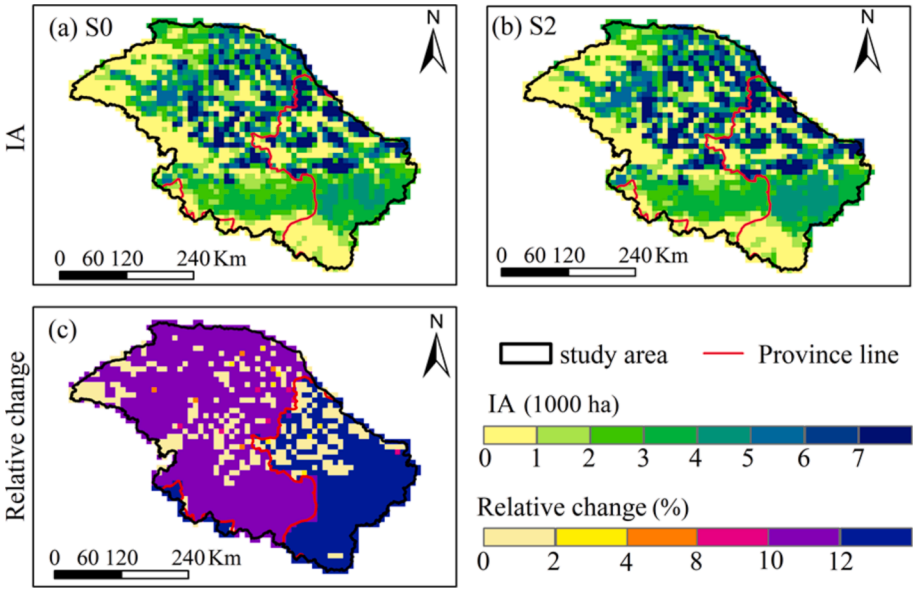

Fig. 14. The IA in S0 and S2 for 2019 and its comparison. The relative change in the figure is the percentage change (%) of the IA in S2 compared to the IA in S0.

water-intensive crops, as the PCR-GLOBWB 2.0 model cannot account for a shift to crops with higher water consumption, which is a limitation of the model that may cause the scenarios to deviate from reality. A promising way to determine the allocation of water-intensive crops or the expansion of IA is using the economic decision model (Dury et al., 2012; Lankford, 2023). Therefore, future work could combine hydrological models (e.g., PCR-GLOBWB 2.0 model) with economic decision models or incorporate the method of economic crop decision into the scheme of irrigation water use simulation of hydrological models to better consider changes in crop planting structure or the expansions of IA.

5. Conclusion

To save water for irrigation, it is a common practice to implement a water-saving policy for increasing IE involving measures such as canal lining and drip irrigation. This study used PCR-GLOBWB 2.0 model to simulate different water-saving scenarios (e.g., increase IE or IA) to evaluate the effects of processes related to the paradox of IE, and to identify the potential effects of irrigation water-saving interventions on the occurrence of hydrological drought in the Huaihe River Basin. The results show that the impact of increasing IE alone on hydrological drought has two-sided effects: aggravation and alleviation. When water availability (WA) is high and can meet most of the crop net water demand (NWD) and the crop gross water demand (GWD), there is a situation in which the decrease of irrigation water withdrawal (IWW) is higher than the increase of irrigation water consumption (IWC) after increasing IE. In this situation, increasing IE alleviates the hydrological drought as intended. However, when water resources are relatively scarce with limited WA and cannot meet most of the NWD and GWD, there is a situation in which the increase of IWC is higher than the decrease of IWW after increasing IE. In this situation, increasing IE leads to the paradox of IE and consequently aggravates the hydrological drought. Also, increasing IE could aggravate the hydrological drought in water-receiving areas as it reduces the water supply from outside regions. The results show that the impacts of increasing IE and IA simultaneously on hydrological drought are also two-sided. However, the aggravating effect is dominant due to the increase in IA leading to a significant increase of IWC and IWW. Notably, when the increase of IA is restricted by the irrigation system, the intensification effect of increasing IE and IA on hydrological drought will be weakened. Meanwhile, when the IA cannot increase or only slightly, increasing IE and IA can result in the decrease of IWW being more significant than the increase of IWC and consequently alleviates hydrological drought. Those findings have important implications for irrigation water regulation in areas with a high intensity of water resource development.

CRediT authorship contribution statement

Hui Cheng: Writing – review & editing, Writing – original draft, Visualization, Validation, Software, Resources, Project administration, Methodology, Investigation, Funding acquisition, Formal analysis, Data curation, Conceptualization. **Wen Wang:** Writing – review & editing, Supervision, Software, Project administration, Methodology, Investigation, Funding acquisition, Formal analysis, Conceptualization. **Inge de Graaf:** Writing – review & editing, Software, Methodology, Conceptualization. **Jingxuan Lu:** Writing – review & editing, Supervision, Methodology, Conceptualization. **Saskia van der Kooij:** Writing – review & editing, Software, Methodology, Conceptualization. **Jeroen Vos:** Writing – review & editing, Software, Methodology, Conceptualization. **Yuan Yao:** Writing – review & editing, Visualization, Software, Methodology, Data curation, Conceptualization. **Pieter van Oel:** Writing – review & editing, Visualization, Supervision, Software, Methodology, Formal analysis, Data curation, Conceptualization.

Declaration of competing interest

The authors declare that they have no known competing financial interests or personal relationships that could have appeared to influence the work reported in this paper.

Acknowledgment

This research was supported by the National Key Research and Development Program of China, China (No. 2023YFC3209201), National Natural Science Foundation of China, China (Grant No. 42471027), Postdoctoral Research Funding Project of Henan Province, China (Grant No. HN2024179), and European Research Council (ERC) under the grant agreement GROW-101041110. Most of the analysis of this work was done during the first author's visit to Wageningen University in 2021-2022.

Data availability

The data that has been used is confidential.

References

Abd El-Wahed, M.H., Medici, M., Lorenzini, G., 2016. Sprinkler irrigation uniformity: impact on the crop yield and water use efficiency. J. Engin. Thermophys. 25, 117–125. https://doi.org/10.1134/S1810232816010112.

Aghakouchak, A., Mirchi, A., Madani, K., Di Baldassarre, G., Nazemi, A., Alborzi, A., Anjileli, H., Azarderakhsh, M., Chiang, F., Hassanzadeh, E., Huning, L.S., Mallakpour, I., Martinez, A., Mazdiyasni, O., Moftakhari, H., Norouzi, H., Sadegh, M., Sadeqi, D., Van Loon, A.F., Wanders, N., 2021. Anthropogenic drought: definition, challenges, and opportunities. Rev. Geophys. 59 (2). https://doi.org/10.1029/2019RG000683.

Alcott, B., 2005. Jevons' paradox. Ecol. Econ. 54 (1), 9–21. https://doi.org/10.1016/j.ecolecon.2005.03.020.

Berbel, J., Gutiérrez-Martín, C., Rodríguez-Díaz, J.A., Camacho, E., Montesinos, P., 2015. Literature review on rebound effect of water saving measures and analysis of a Spanish case study. Water Resour. Manage. 29, 663–678. https://doi.org/10.1007/s11269-014-0839-0.

Birkenholtz, T., 2017. Assessing India's drip-irrigation boom: efficiency, climate change and groundwater policy. Water Int. 42 (6), 663–677. https://doi.org/10.1080/02508060.2017.1351910.

Burek, P., Satoh, Y., Kahil, T., Tang, T., Greve, P., Smilovic, M., Guillaumot, L., Zhao, F., Wada, Y., 2020. Development of the Community Water Model (CWatM v1.04) – a high-resolution hydrological model for global and regional assessment of integrated water resources management. Geosci. Model Dev. 13, 3267–3298. https://doi.org/10.5194/gmd-13-3267-2020.

Chen, X., Wang, Z., Hu, J., Wang, Z., 2013. Analysis of Drought characteristics in the Huaihe River basin in recent 60 years (in Chinese). South-to-North Water Diversion Water Conservancy Sci. Technol. 11 (6), 20–24. https://doi:10.3724/SP.J.1201.2013.06020.

Cheng, H., Wang, W., van Oel, P.R., Lu, J., Wang, G., Wang, H., 2021. Impacts of different human activities on hydrological drought in the Huaihe River Basin based on scenario comparison. J. Hydrol-Reg. Stud. 37, 100909. https://doi.org/10.1016/j.ejrh.2021.100909.

Contor, B.A., Taylor, R.G., 2013. Why improving irrigation efficiency increases total volume of consumptive use. Irrig. Drain. 62 (3), 273–280. https://doi.org/10.1002/ird.1717.

de Graaf, I.E.M., Van Beek, L.P.H., Wada, Y., Bierkens, M.F.P., 2014. Dynamic attribution of global water demand to surface water and groundwater resources: effects of abstractions and return flows on river discharges. Adv. Water Resour. 64, 21–33. https://doi.org/10.1016/j.advwatres.2013.12.002.

de Graaf, I.E.M., Gleeson, T., Rens Van Beek, L.P.H., Sutanudjaja, E.H., Bierkens, M.F.P., 2019. Environmental flow limits to global groundwater pumping. Nature 574 (7776), 90–94. https://doi.org/10.1038/s41586-019-1594-4.

Döll, P., Siebert, S., 2002. Global modeling of irrigation water requirements. Water Resour. Res. 38 (4), 8-1–8-10. https://doi.org/10.1029/2001WR000355.

Droppers, B., Franssen, W.H.P., Van Vliet, M.T.H., Nijssen, B., Ludwig, F., 2020. Simulating human impacts on global water resources using VIC-5. Geosci. Model Dev. 13 (10), 5029–5052. https://doi.org/10.5194/gmd-13-5029-2020.

Dury, J., Schaller, N., Garcia, F., Reynaud, A., Bergez, J.E., 2012. Models to support cropping plan and crop rotation decisions. A review. Agron. Sustain. Dev. 32, 567–580. https://doi.org/10.1007/s13593-011-0037-x.

Espinosa-Tasón, J., Berbel, J., Gutiérrez-Martín, C., 2020. Energized water: evolution of water-energy nexus in the Spanish irrigated agriculture, 1950–2017. Agric. Water Manage. 233, 106073. https://doi.org/10.1016/j.agwat.2020.106073.

FAO., 2017. Does Improved Irrigation Technology Save Water? A Review of the Evidence. Discussion paper on irrigation and sustainable water resources management in the Near East and North Africa. Food and Agriculture Organisation (FAO), Rome.

Grafton, R.Q., Williams, J., Perry, C.J., Molle, F., Ringler, C., Steduto, P., Udall, B., Wheeler, S.A., Wang, Y., Garrick, D., Allen, R.G., 2018. The paradox of irrigation efficiency. Science 361 (6404), 748–750. https://doi.org/10.1126/science.aat9314.

He, X., Wada, Y., Wanders, N., Sheffield, J., 2017. Intensification of hydrological drought in California by human water management. Geophys. Res. Lett. 44 (4), 1777–1785. https://doi.org/10.1002/2016GL071665.

He, J., Yang, K., Tang, W., Lu, H., Qin, J., Chen, Y.Y., Li, X., 2020. The first high-resolution meteorological forcing dataset for land process studies over China. Sci. Data 7, 25. https://doi.org/10.1038/s41597-020-0369-y.

Huang, Z., Hejazi, M., Li, X., Tang, Q., Vernon, C., Leng, G., Liu, Y., Döll, P., Eisner, S., Gerten, D., Hanasaki, N., Wada, Y., 2018. Reconstruction of global gridded monthly sectoral water withdrawals for 1971–2010 and analysis of their spatiotemporal patterns. Hydrol. Earth Syst. Sci. 22, 2117–2133. https://doi.org/10.5194/hess-22-2117-2018.

Huang, Q., Wang, J., Li, Y., 2017. Do water saving technologies save water? Empirical evidence from North China. J. Environ. Econ. Manag. 82, 1–16. https://doi.org/10.1016/j.jeem.2016.10.003.

Ilyas, A., Manzoor, T., Muhammad, A., 2021. A dynamic socio-hydrological model of the irrigation efficiency paradox. Water Resour. Res. 57 (12). https://doi.org/10.1029/2021WR029783.

Irmak. S., Odhiambo, L.O., Kranz, W.L., Eisenhauer, D.E. 2011. Irrigation efficiency and uniformity, and crop water use efficiency. University of Nebraska–Lincoln Extension.

Lankford, B.A., 2023. Resolving the paradoxes of irrigation efficiency: Irrigated systems accounting analyses depletion-based water conservation for reallocation. Agric. Water Manage. 287, 108437. https://doi.org/10.1016/j.agwat.2023.108437.

Lankford, B., Closas, A., Dalton, J., Gunn, E.L., Hess, T., Knox, J.W., van der Kooij, S., Lautze, J., Molden, D., Orr, S., Pittocki, J., Richter, B., Riddell, P.J., Scott, C.A., Venot, J.P., Vos, J., Zwarteveen, M., 2020. A scale-based framework to understand the promises, pitfalls and paradoxes of irrigation efficiency to meet major water challenges. Global Environ. Chang. 65, 1–24. https://doi.org/10.1016/j.gloenvcha.2020.102182.

Li, X., Jiang, W., Duan, D., 2020. Spatio-temporal analysis of irrigation water use coefficients in China. J. Environ. Manage. 262, 110242. https://doi.org/10.1016/j.jenvman.2020.110242.

Liu, Y., Tian, F., 2016. Comparison of water and land policies for agriculture water conservation in arid areas based on a coupled socio-hydrological model (In Chinese). I Tsinghua Univ. (Sci. Technol.). 56 (4), 365–372. https://doi.org/10.16511/j.cnki.qhdxxb.2016.24.005.

López López, P., Sutanudjaja, E.H., Schellekens, J., Sterk, G., Bierken, M.F.P., 2017. Calibration of a large-scale hydrological model using satellite-based soil moisture and evapotranspiration products. Hydrol. Earth Syst. Sci. 21 (6), 3125–3144. https://doi.org/10.5194/hess-21-3125-2017.

McVeigh, M., Wyllie, A., 2018. Memo on irrigation efficiency and ESPA storage changes. State of Idaho Department of Water Resources, 5.

Molle, F., Tanouti, O., 2017. Squaring the circle: agricultural intensification vs. water conservation in Morocco. Agric. Water Manage. 192, 170–179. https://doi.org/10.1016/j.agwat.2017.07.009.

Perry, C.J., Steduto, P., Karajeh, F., 2017. Does Improved Irrigation Save Water? A Review of the Evidence. Food and Agriculture Organization of the United Nation, Cairo.

Ruijsch, J., Verstegen, J.A., Sutanudjaja, E.H., Karssenberg, D., 2021. Systemic change in the Rhine-Meuse basin: quantifying and explaining parameters trends in the PCR-GLOBWB global hydrological model. Adv. Water Resour. 155, 104013. https://doi.org/10.1016/j.advwatres.2021.104013.

Schilstra, M., Wang, W., van Oel, P.R., Wang, J., Cheng, H., 2024. The effects of reservoir storage and water use on the upstream–downstream drought propagation. J. Hydrol. 631, 130668. https://doi.org/10.1016/j.jhydrol.2024.130668.

Scott, C.A., Vicuña, S., Blanco-Gutiérrez, I., Meza, F., Varela-Ortega, C., 2014. Irrigation efficiency and water-policy implications for river basin resilience. Hydrol. Earth Syst. Sci. 18, 1339–1348. https://doi.org/10.5194/hess-18-1339-2014.

Sese-Minguez, S., Boesveld, H., Asins-Velis, S., Van der Kooij, S., Maroulis, J., 2017. Transformations accompanying a shift from surface to drip irrigation in the Cànyoles Watershed, Valencia, Spain. Water Alternatives 10 (1), 81.

Stott, P., 2016. How climate change affects extreme weather events. Science 352 (6293), 1517–1518. https://doi.org/10.1126/science.aaf7271.

Sutanudjaja, E.H., Beek, L.P.H.V., Jong, S.M.D., Van Geer, F.C., Bierkens, M.F.P., 2014. Calibrating a large extent high-resolution coupled groundwater and surface model using soil moisture and discharge data. Water Resour. Res. 50 (1), 687–705. https://doi.org/10.1002/2013WR013807.

Sutanudjaja, E.H., Beek, R.V., Wanders, N., Wada, Y., Bosmans, J.H.C., Drost, N., Van, d. E.R.J., De Graaf, I.E.M., Hoch, J.M., De Jong, K., Karssenberg, D., Lopez Lopez, P., Peßenteiner, S., Schmitz, O., Straatsma, M.W., Vannametee, E., Wisser, D., Bierkens, M.F.P., 2018. PCR-GLOBWB 2: a 5 arcmin global hydrological and water resources model. Geosci. Model Dev. 11 (6), 2429–2453. https://doi.org/10.5194/gmd-11-2429-2018.

Van Beek, L.P.H., Wada, Y., Bierkens, M.F.P., 2011. Global monthly water stress: 1. Water balance and water availability. Water Resour. Res. 47, W07517. https://doi.org/10.1029/2010WR00979.

van der Kooij, S., Zwarteveen, M., Boesveld, H., Kuper, M., 2013. The efficiency of drip irrigation unpacked. Agric. Water Manage. 123, 103–110. https://doi.org/10.1016/j.agwat.2013.03.014.

Van Halsema, G.E., Vincent, L., 2012. Efficiency and productivity terms for water management: a matter of contextual relativism versus general absolutism. Agric. Water Manage. 108, 9–15. https://doi.org/10.1016/j.agwat.2011.05.016.

van Langen, S.C.H., Costa, A.C., Ribeiro Neto, G.G., van Oel, P.R., 2021. Effect of a reservoir network on drought propagation in a semi-arid catchment in Brazil. Hydrol. Sci. J. 66 (10), 1567–1583. https://doi.org/10.1080/02626667.2021.1955891.

Van Loon, A.F., Gleeson, T., Clark, J., Dijk, A.V., Stahl, K., Hannaford, J., Baldassarre, G. D., Teuling, A.J., Tallaksen, L.M., Uijlenhoet, R., Hannah, D.M., Sheffield, J., Svoboda, M., Verbeiren, B., Wagener, T., Rangecroft, S., Wanders, N., Van Lanen, H. A.J., 2016. Drought in the anthropocene. Nat. Geosci. 9 (2), 89–91. https://doi.org/10.1038/ngeo2646.

Van Loon, A.F., Rangecroft, S., Coxon, G., Werner, M., Wanders, N., Di Baldassarre, G., Tijdeman, E., Bosman, M., Gleeson, T., Nauditt, A., Aghakouchak, A., Breña-Naranjo, J.A., Cenobio-Cruz, O., Costa, A.C., Fendekova, M., Jewitt, G., Kingston, D. G., Loft, J., Mager, S.M., Mallakpour, I., Masih, I., Maureira-Cortés, H., Toth, E., Van Oel, P., Van Ogtrop, F., Verbist, K., Vidal, J., Wen, L., Yu, M., Yuan, X., Zhang, M., Van Lanen, H.A.J., 2022. Streamflow droughts aggravated by human activities despite management. Environ. Res. Lett. 17 (4), 44059. https://doi.org/10.1088/1748-9326/ac5def.

Van Oel, P.R., Martins, E.S., Costa, A.C., Wanders, N., Van Lanen, H.A.J., 2018. Diagnosing drought using the downstreamness concept: the effect of reservoir networks on drought evolution. Hydrol. Sci. J. 63 (7), 979–990. https://doi.org/10.1080/02626667.2018.1470632.

Wada, Y., Van Beek, L.P., Wanders, N., Bierkens, M.F., 2013. Human water consumption intensifies hydrological drought worldwide. Environ. Res. Lett. 8 (3), 034036. https://doi.org/10.1088/1748-9326/8/3/034036.

Wada, Y., Wisser, D., Bierkens, M.F.P., 2014. Global modeling of withdrawal, allocation and consumptive use of surface water and groundwater resources. Earth Syst. Dyn. 5, 15–40. https://doi.org/10.5194/esd-5-15-2014.

Wanders, N., Wada, Y., 2015. Human and climate impacts on the 21st century hydrological drought. J. Hydrol. 526, 208–220. https://doi.org/10.1016/j.jhydrol.2014.10.047.

WorldPop (www.worldpop.org - School of Geography and Environmental Science, University of Southampton; Department of Geography and Geosciences, University of Louisville; Departement de Geographie, Universite de Namur) and Center for International Earth Science Information Network (CIESIN), Columbia University (2019). Global High Resolution Population Denominators Project - Funded by The Bill and Melinda Gates Foundation (OPP1134076). https://dx.doi.org/10.5258/SOTON/WP00675.

Xiong, R., Zheng, Y., Han, F., Tian, Y., 2021. Improving the scientific understanding of the paradox of irrigation efficiency: an integrated modeling approach to assessing basin-scale irrigation efficiency. Water Resour. Res. 57. https://doi.org/10.1029/2020WR029397.

Yang, X., Zhang, M., He, X., Ren, L., Pan, M., Yu, X., Wei, Z., Sheffield, J., 2020. Contrasting influences of human activities on hydrological drought regimes over China based on high-resolution simulations. Water Resour. Res. 56. https://doi.org/10.1029/2019WR025843.

Zhang, L., Ren, Z., Chen, B., Gong, P., Fu, H., Xu, B. 2021. A Prolonged Artificial Nighttime-light Dataset of China (1984-2020). National Tibetan Plateau Data Center, DOI: 10.11888/Socioeco.tpdc.271202. CSTR: 18406.11.Socioeco.tpdc.271202.

Zhang, X., Hao, Z., Singh, V.P., Zhang, Y., Feng, S., Xu, Y., Hao, F., 2022b. Drought propagation under global warming: characteristics, approaches, processes, and controlling factors. Sci. Total Environ. 156021. https://doi.org/10.1016/j.scitotenv.2022.156021.

Zhang, L., Zheng, D., Zhang, K., Chen, H., Ge, Y., Li, X., 2022a. Divergent trends in irrigation-water withdrawal and consumption over mainland China. Environ. Res. Lett. 9 (17), 1–13. https://doi.org/10.1088/1748-9326/ac8606.

Zhou, F., Bo, Y., Ciais, P., Dumas, P., Tang, Q., Wang, X., Liu, J., Zheng, C., Polcher, J., Yin, Z., Guimberteau, M., Peng, S., Ottle, C., Zhao, X., Zhao, J., Tan, Q., Chen, L., Shen, H., Yang, H., Piao, S., Wang, H., Wada, Y., 2020. Deceleration of China's human water use and its key drivers. Proc. Natl. Acad. Sci. USA 117 (14), 7702–7711. https://doi.org/10.1073/pnas.1909902117.